Theory of the polarization dependence of reactive collisions and its application to the associative ionization process $2Na(3\,^2P_{3/2}) \rightarrow Na_2^+(X\,^2\Sigma_g^+) + e^-$

Dumont M. Jones and John S. Dahler
Departments of Chemistry and Chemical Engineering, University of Minnesota, Minneapolis, Minnesota 55455
(Received 27 October 1986)

We consider collisions between (quasi-) one- or two-electron atoms, each of which has been prepared in a fixed distribution of hyperfine magnetic substates. The resulting "polarization-dependent" reaction rates are functions of (1) the (experimentally adjustable) orientation of the quantization axis associated with the hyperfine substates, (2) the hyperfine terms of the colliding atoms, and (3) the detailed reaction dynamics as characterized by preparation- and fine-structure-independent cross sections. These effects are deconvoluted and analyzed, and their use in elucidating reaction mechanisms is discussed. Particular emphasis is placed on the associative ionization of two Na($3p$) atoms, each prepared by adsorption of resonant laser photons. The quasimolecular states of Na $\cdots$ Na that might react in this case are limited by selection rules. More information on the reaction mechanism is then obtained by using experimental data, in combination with the formal analysis, to draw further conclusions about the active quasimolecular states.

I. INTRODUCTION

The theory presented in this paper is designed to aid in analyzing measurements of the reaction rates of atoms, the electronic orbitals of which have been oriented prior to collision. The orientation or "polarization" dependence of the rates is intrinsically interesting; it also can be used as a tool for investigating reaction mechanisms. Our goal is to establish the connections between the mechanisms of reactive collisional events and the polarization dependence of experimentally determined rates of reaction. Although much of the theory presented here is directly applicable or easily adapted to a variety of situations, focus is lent to the presentation by keeping in mind a specific prototypical process. The particular case to which we repeatedly shall refer is the associative ionization of two colliding atoms which have been excited into reactive electronic states by polarized lasers. Kircz, Morgenstern, and Nienhuis[1] were the first to report on how the rate of a process such as this varied with the angle β between the direction of laser polarization and the direction of the relative velocity of the colliding atoms. Their observations subsequently were confirmed by Hertel[2] and his coworkers and by Rothe[3] and his collaborators. In these experiments a linearly polarized Na D_2-line laser pumps the $F=2 \rightarrow F=3$ hyperfine transition between the $3\,^2S_{1/2}$ ground state and the $3\,^2P_{3/2}$ excited states of sodium. This laser is arranged so that it intersects an effusive oven beam of atomic sodium at right angles. Subthermal collisions between pairs of excited atoms occur because of the axial dispersion of the beam. The diatomic ions produced by the reaction

$$2Na(3\,^2P_{3/2}) \rightarrow Na_2^+(X\,^2\Sigma_g^+) + e^- \tag{1.1}$$

are then collected and counted.

The pumping process prepares the atoms in an anisotropic distribution of magnetic hyperfine substates, consisting (in the stationary limit) of five ($M_F=0,\pm1,\pm2$) for the case of linear polarization and of only one ($M_F=+3$ or $M_F=-3$) for the case of circular polarization. The projection quantum numbers appearing here are referred to the "photon frame," the polar axis of which coincides with the laser polarization axis in the first case and with the direction of photon propagation in the second. The delicate aspects of atomic structure which are needed for characterizing the hyperfine states populated by the preparative laser play no significant role in the dynamics of the subsequent collisional chemiionization. The rates of these events can be described accurately and efficiently in terms of transitions between quasimolecular adiabatic (or diabatic) Born-Oppenheimer (ABO) states of pairs of reactant atoms and, in the case of Penning ionization, the analogously defined states of the ionic products. Therefore, what one must learn is how to transform information about the populations of the atomic hyperfine states (referred to the laser photon frame) into information about the populations of the ABO initial states [referred to a "laboratory frame" determined by the orientation(s) of the atomic beam(s)]. By convoluting the latter with scattering amplitudes specific to individual quasimolecular ABO initial states, one then can produce rate expressions appropriate for comparison with experimental observations. It is obvious but remarkable, nevertheless, that these individual scattering amplitudes are basic components which can be compounded to conform to a variety of experimental arrangements, each represented by a different initial-state density operator.

One of our goals is to extract numerical estimates of state-to-state cross sections from a knowledge of the experimental reaction rate and of the initial-state density

matrix. The procedure for doing this is illustrated by the following considerations. When the angle between the laser polarization and the direction of relative motion of the colliding atoms is equal to zero, the sodium p orbitals tend to lie along the beam axis, whereas $\beta=\pi/2$ favors p orbitals oriented perpendicular to the beam. One might expect these two arrangements to favor the formation of σ and π bonds, respectively, with the relative populations of the quasimolecular Na_2 initial states controlled by altering the value of β. Thus, it is expected that the rate of associative ionization will depend upon this angle and, indeed, the rate of production of Na_2^+ ions is observed to diminish by as much as 40% when β varies from 0 to $\pi/2$. Experimental observations for two values of the beam's average relative velocity are shown in Fig. 1.

One expects on intuitive grounds that the integral cross section appropriate to this experiment can be written in the form

$$\sigma(E,\beta)=\sum_p \sigma_{pp}(E)\rho_{pp}(\beta) \tag{1.2}$$

with the labels p indicating quasimolecular states of reactant atomic pairs and E the mean kinetic energy of their relative motion. Here $\sigma_{pp}(E)$ denotes the cross section specific to the quasimolecular state p and $\rho_{pp}(\beta)$ the corresponding element of the density matrix. The angle (β) dependence of the latter accounts for the difference between the polarization axis of the preparative laser and the direction of relative motion of the colliding atoms. If $\sigma(E,\beta)$ and the set of density operator components $\rho_{pp}(\beta)$ are known, (1.2) can be used to constrain the possible values of the cross sections $\sigma_{pp}(E)$. This is the basic idea underlying the calculations in Sec. VI.

In a previous paper[4] (henceforth referred to as I) we used conventional quantal theories of associative ionization to obtain a formula similar to (1.2) but augmented by "off-diagonal" terms $\sigma_{pp'}\rho_{pp'}$ ($p'\neq p$) which were bilinear with respect to transition amplitudes associated with two different quasimolecular initial states. Many but not all of these interference cross terms were then found to be zero, either because of dynamic selection rules (properties of the objects $\sigma_{pp'}$) or because off-diagonal elements of the initial-state density matrix were zero due to symmetries of the preparative procedure. Although most of the cross-section selection rules were quite rigorous, one was obtained using an approximation which has been an integral part of most theories of ionizing collisions,[5] including our own generalizations of these theories to laser-induced chemiionization[6] and excitation transfer.[7] According to this approximation, off-diagonal matrix elements of the transition operator connecting states with different rigid-rotor angular momentum quantum numbers, L and L', are assumed not to differ significantly in value from the corresponding diagonal elements. Although it is unlikely that this approximation adversely affects calculations of the heavy-particle motions, which usually involve relatively large rotational quantum numbers, it is less certain that it can be trusted to produce a valid selection rule for the electronic angular momentum quantum number Λ, which rarely assumes values other than 0, 1, or 2. Recently we have succeeded in deriving an almost equivalent selection rule without recourse to this questionable approximation, cf. Sec. II C.

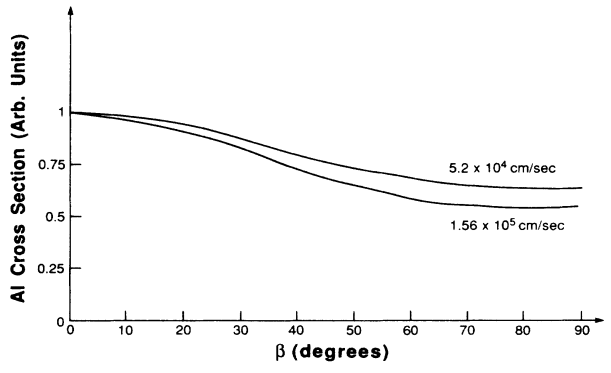

FIG. 1. Dimensionless cross section $\sigma(E,\beta)/\sigma(E,0)$ for the associative ionization process $2Na[^2P_{3/2}(3p)]\rightarrow Na_2^+(X\,^2\Sigma_g^+)+e^-$, after Ref. 2. β is the angle between the electric field vector of the preparative laser and the direction of initial relative velocity.

Another of the selection rules requires for its implementation qualitative information about the shapes of the adiabatic (diabatic) energy curves associated with the quasimolecular states of Na_2. In particular, one must know whether and where these curves intersect that of the product $Na_2^+(X\,^2\Sigma_g^+)$ diatomic ion. At the time when paper I was written a potential energy curve was available for only one of the excited electronic states that were possible contributors to the experimentally observed rate of associative ionization, namely, the lowest-lying $^1\Sigma_g^+$ state which correlates asymptotically with $Na(3p)+Na(3p)$. The results of our analysis of the experimental data depended critically on this one potential energy curve, which subsequently was found to be seriously in error, cf. the dotted curve of Fig. 3. The analysis presented here makes use of more recent and presumably more reliable information about these energy curves.

The presence or absence of "interference cross sections" is a delicate issue which requires proof and not simple assertion. In writing (1.2) we referred to "intuitive grounds" for expecting that there would be no interference contributions when the colliding pairs of atoms were classified according to quasimolecular ABO states. This expectation may be more a reflection of conventional wisdom or habit than of sound fundamentals, but we have succeeded in *proving* that it is a good approximation for the specific situations treated here. To illustrate the pitfalls of which one must be wary, let us assume that (1.2) has indeed been proved. We then consider a different labeling of the two-atom precollision states, indicated by the Latin indices $i=1,2,\ldots$. It would *not* be correct to assert that $\sigma_{ii'}\propto\delta_{ii'}$, cf. Sec. II C. In particular, there generally will be nonzero interference cross section $\sigma_{ii'}$ ($i\neq i'$) for a basis consisting of direct products of atomic states labeled with quantum numbers such as (L,M_L,S,M_S),[8] (L,S,J,M_J) (Refs. 1 and 9) or (L,S,I,F,M_F). It is therefore our contention that interference cross sections cannot be assigned zero values unless there are solid, fundamental reasons for

doing so. Simple intuitive arguments do not suffice and studies[1,8,9] which ignore interference terms from the outset will reach conclusions of uncertain validity.

The theory of paper I has been considerably refined, amended, and corrected. In particular, the cross-section selection rules have been revised and placed on firm fundamental foundations. Also, a much more powerful diagrammatic method has been used to perform the angular momentum manipulations needed for constructing the density matrix of quasimolecular precollision states from a knowledge of the laser-prepared atomic beam(s). This part of the theory is quite general and not at all restricted in its applicability to associative ionization. To appreciate the complexity of the problem one must recognize that the angular momenta of the states populated by the preparative laser are sums $\mathbf{F}=\mathbf{I}+\mathbf{J}=\mathbf{I}+(\mathbf{L}+\mathbf{S})$ of three angular momenta and that the density operator pertains to two such atoms. What the evaluation of the density matrix entails is a recoupling of these six angular momenta into the composite electron spin and orbital angular momentum of the two atoms as well as a sum (the taking of a trace) over the collisionally irrelevant nuclear spins. Complications arise when the nuclei are identical for then the nuclear statistics impose symmetry restrictions on the wave functions descriptive of the heavy-particle motions [for example, recall the restrictions on the rotational quantum numbers of orthohydrogen and parahydrogen].

The coupling of two angular momenta involves a $3j$ symbol and the coupling of three requires $6j$ symbols. When six angular momenta are involved, $15j$ symbols can enter the picture. This does, in fact, occur when one transforms the density matrix from the atomic basis to the molecular basis. Furthermore, it should be remembered that the photon and collision (laboratory) frames are not the same, so that rotational transformations also must be taken into account. It is for problems with this degree of complexity that the diagrammatic techniques are highly desirable if not wholly indispensable. The density matrix has invariants and symmetries and the various angular momenta conform to a number of constraints, such as triangle rules. The diagrammatic procedure delicately extracts these important characteristics from the jungle of algebraic complexity associated with the recoupling of so many angular momenta. This analysis of the density matrix is an important component of the theory of laser-prepared atomic collisions to which little attention previously has been directed. Indeed, the only studies of which we are aware are those of Hertel and co-workers[10] and Nienhuis,[9] both of whom limited their studies to direct-product states of independent (distinguishable) atoms instead of the diatomic, ABO states to which the generalized cross sections $\sigma_{p'p''}(E)$ are related.

The plan of the paper is as follows. Section II provides a detailed formal treatment of the density operator appropriate to a pair of laser-prepared atoms. The matrix elements of this operator are then combined with elements of the transition operator to produce formulas for reactive associative-ionization cross sections. Results are presented for both identical and distinguishable nuclei. Section II C is devoted to cross-section selection rules, some of which are specific to associative ionization and some of which are not. Section III is a brief summary of the notation and methods associated with the diagrammatic techniques for handling the algebra of angular momenta. In Sec. IV these techniques are used to derive a compact, general formula for the density matrix of quasimolecular, laser-prepared precollision states. This formula is used in Sec. V to produce a number of symmetry-related predictions about the cross sections for polarization-dependent collision processes. At the end of Sec. V, we comment upon how the theory presented to that point can be applied to other processes. In Sec. VI the theory of the preceding sections is applied to the analysis of the experimentally measured, polarization-dependent associative ionization of two $\mathrm{Na}(3\,^2P_{3/2})$ atoms. The paper ends with a summary, some conclusions, and a few comments about future experiments and theory in this general area of research.

II. RESULTS FROM THE THEORY OF ASSOCIATIVE IONIZATION

In this section we present results from the theory of associative ionization (AI) that are needed for analyzing the experimentally observed laser polarization dependence of the rates of processes such as $2\mathrm{Na}((3p)^2P_{3/2}) \rightarrow \mathrm{Na}_2{}^+(X\,^2\Sigma_g^+)+e^-$. The first item to be considered is the density operator associated with the initial laser-prepared state of a beam atom. The theoretical cross section corresponding to the measured rate of AI is then expressed in terms of state-specific cross sections σ_{pp} and "interference cross sections" $\sigma_{pp'}$ $(p\neq p')$, all of which are independent of the laser polarization, and a *polarization-dependent* density operator $\rho_{pp'}(\alpha,\beta)$. The labels p and p' appearing here refer to quasimolecular electronic states that are descriptive of the state of the system prior to collisional ionization. The angles α and β are the first and second Euler angles (equal to the polar spherical coordinates ϕ and θ, respectively). These specify the direction of $\hat{\boldsymbol{\alpha}}$, the "photon-frame" space-quantization axis measured relative to a laboratory-fixed frame. In the case of linear polarization, $\hat{\boldsymbol{\alpha}}$ is coincident with the polarization axis of the laser; for circular polarization it is parallel to the direction of the laser beam.[11] The analysis presented here is specific to a single laser or to two which share a common photon frame. The extension to lasers with different photon frames will be presented separately.

The representation of the AI reaction rate in terms of quasimolecular state-specific cross sections and the corresponding density operator is done first without regard for nuclear statistics and then again allowing for the indistinguishability of identical atomic nuclei. General formulas are reported for the cross sections and density matrix. (In Sec. IV the density matrix is expressed in terms of readily computable objects such as $6j$ symbols. This computation is not specific to AI and can be applied to a general atomic reaction.) Finally, we report "selection rules" that greatly diminish the number of nonzero off-diagonal cross sections $\sigma_{pp'}$ $(p\neq p')$, thereby enabling a more precise identification of the quasimolecular states of the reactant atoms which contribute to the measured rate of reaction. Details omitted here can be found either in a previ-

ous paper[4] or in a forthcoming communication on the theory of chemiionization.[12]

A. Initial-state density operators

The events that concern us involve pairs of atoms X and Y, excited into hyperfine states $|n\rangle$ and $|n'\rangle$, respectively, by the resonant absorption of single-mode cw laser radiation. The gas density and the intensity and spot size of the laser(s) are assumed to be such that each atom interacts with many photons before striking another. Consequently, the density operators specific to the electronic and nuclear spin states of these atoms may be written in the forms

$$\rho_X=\sum_n P_X(n)\,|n\rangle\langle n|\ , \tag{2.1}$$

$$\rho_Y=\sum_{n'} P_Y(n')\,|n'\rangle\langle n'|\ , \tag{2.2}$$

with $P_X(n)$ and $P_Y(n')$ denoting the probabilities of finding atom X in the state $|n\rangle$ and Y in the state $|n'\rangle$. Details about these hyperfine states are given in Sec. IV.

We distinguish between two types of (initial) atomic kets. The first (of which the angular brackets $|n\rangle$ and $|n'\rangle$ are examples) have the photon-frame quantization axis $\hat{\alpha}$, with Euler angles $(\alpha,\beta,0)$. The second type, represented by rounded brackets as $|n)$ and $|n')$, have a space-quantization axis which points in the direction of the initial relative momentum $\hbar\mathbf{k}=\hbar[(\mu/m_X)\mathbf{k}_X-(\mu/m_Y)\mathbf{k}_Y]$ of the two colliding atoms. Here, $\hbar\mathbf{k}_X$ and $\hbar\mathbf{k}_Y$ are the atomic momenta, m_X and m_Y the atomic masses, and $\mu^{-1}=m_X^{-1}+m_Y^{-1}$. These two sets of kets are connected by the relationships

$$|n\rangle=\underline{R}(\hat{\alpha})\,|n)\ , \tag{2.3}$$

$$|n'\rangle=\underline{R}'(\hat{\alpha})\,|n')\ , \tag{2.4}$$

with the operator $\underline{R}(\hat{\alpha})$ denoting an active rotation on the state space of atom X and $\underline{R}'(\hat{\alpha})$ a similarly defined operator specific to atom Y. As indicated in (2.3) and (2.4), the quantum numbers associated with the two kets $|n)$ and $|n\rangle$, including projections of angular momentum, are numerically equal.

Throughout this paper initial internal states will be represented by angular or rounded brackets, whichever is appropriate, and by small *Latin* letters. The internal states of the product XY^+ ions will be denoted by angular brackets (which have no special significance in this case) and small *Greek* letters.

Because the probabilities $P_X(n)$ and $P_Y(n')$ do not depend on the direction $\hat{\alpha}$, the density operators given by (2.1) and (2.2) may be rewritten in the alternative forms

$$\rho_X=\sum_n P_X(n)\underline{R}(\hat{\alpha})\,|n)(n\,|\,\underline{R}^{\dagger}(\hat{\alpha})\ , \tag{2.5}$$

$$\rho_Y=\sum_{n'} P_Y(n')\underline{R}'(\hat{\alpha})\,|n')(n'\,|\,\underline{R}'^{\dagger}(\hat{\alpha})\ . \tag{2.6}$$

It will become apparent that the $\hat{\alpha}$ dependence of the rate of associative ionization is confined completely to the rotation operators $\underline{R}(\hat{\alpha})$ and $\underline{R}'(\hat{\alpha})$.

Finally, we write the density operator for a pair of laser-prepared atoms as

$$\rho=\sum_{n,n'}\underline{A}\,|n\rangle\,|n'\rangle P_X(n)P_Y(n')\langle n\,|\,\langle n'\,|\,\underline{A}^{\dagger}$$
$$=\sum_{n,n'}|i\rangle P_X(n)P_Y(n')\langle i|\ , \tag{2.7}$$

with $|i\rangle\equiv\underline{A}\,|nn'\rangle$ denoting the product state $|nn'\rangle$, antisymmetrized in *all* electronic coordinates. This expression for the initial-state density matrix is appropriate when the states of the atomic reactants have been prepared independently, as they have in the situations considered here.

B. Scattering amplitudes and cross sections for AI

We now consider an AI collisional event beginning with two atoms X and Y in the hyperfine states $|n\rangle$ and $|n'\rangle$, respectively, and moving relative to one another with a momentum equal to $\hbar\mathbf{k}$. The products of reaction consists of an XY^+ ion and a free electron, which travels in the direction $\hat{\mathbf{q}}$ with a momentum $\hbar q$ (measured relative to the XY^+ product ion). The spin of the free electron and the internal state of the diatomic ion are described by a ket $|\gamma\rangle$. The scattering amplitude for this process is written as

$$f^+(\mathbf{q}\gamma;\mathbf{k}nn')=(m_e/2\pi\hbar^2)\langle\mathbf{q}\gamma\,|\,T\,|\,\mathbf{k}nn'\rangle\ , \tag{2.8}$$

with T the transition operator, m_e the electron mass, and $\mathbf{q}\equiv\hat{\mathbf{q}}q$. This scattering amplitude is associated with a process which we write as

$$X(n\,\mathbf{k})+Y(n'\mathbf{k})\rightarrow XY^+(\gamma)+e^-(\mathbf{q})\ .$$

The plus superscript indicates that f^+ is the amplitude associated with the conventionally defined "out" boundary condition of scattering theory. Two points regarding f^+ should be mentioned. The first of these is that f^+ will be computed as if the nuclei were distinguishable, even when they are identical. The consequences of nuclear statistics will be treated separately. Secondly, f^+ is computed using a spin-free, nonrelativistic Hamiltonian. The errors incurred by this approximation will be negligible provided that the electronic spin-orbit coupling is small compared with the other interactions that come into play during the collision. The thing to notice here is that the part of the system Hamiltonian which shapes the scattering amplitude f^+ is far different from that which accounts for the photoabsorptive events that are responsible for populating the atomic hyperfine states prior to collision. Although the electronic and nuclear spins are important contributors to the latter events, they usually have little effect upon the former.

Because the transition matrix notation, $\langle\,|\,T\,|\,\rangle$, is better suited to our needs, we use it in place of the equivalent scattering amplitude notation.

Let us now introduce the transition matrix elements

$$\langle\mathbf{q}\delta\,|\,T\,|\,\mathbf{k}p\rangle\equiv\sum_{\gamma}\sum_{n,n'}\langle\delta\,|\,\gamma\rangle\langle nn'\,|\,p)\langle\mathbf{q}\gamma\,|\,T\,|\,\mathbf{k}nn'\rangle \tag{2.9}$$

and

$$\langle q\lambda\mu\delta \mid T \mid \mathbf{k}p\rangle \equiv \sum_{\gamma}\sum_{n,n'}\int d\hat{\mathbf{q}}\langle\delta \mid \gamma\rangle\langle nn' \mid p\rangle Y^{*}_{\lambda\mu}(\hat{\mathbf{q}})\langle \mathbf{q}\gamma \mid T \mid \mathbf{k}nn'\rangle = \int d\hat{\mathbf{q}}\, Y^{*}_{\lambda\mu}(\hat{\mathbf{q}})\langle \mathbf{q}\delta \mid T \mid \mathbf{k}p\rangle , \tag{2.10}$$

where it is to be understood that $\mid p)$ lies in the same degenerate manifold as $\underline{A} \mid nn'\rangle \equiv \underline{A} \mid n\rangle \mid n'\rangle$ and $\mid\delta\rangle$ in the same degenerate manifold as $\mid\gamma\rangle$. We assume that the states within each of the sets $\mid n\rangle$, $\mid n'\rangle$, $\mid p)$, $\mid\delta\rangle$, and $\mid\gamma\rangle$ are orthonormal.

The symbol λ appearing in (2.3) is the angular momentum quantum number of the free electron and $\mu\hbar$ is the projection of this angular momentum in the direction of $\mathbf{k}=\hat{\mathbf{k}}k$. The kets $\mid p)$ invariably will be identified as "molecular-type" states, which are bases of irreducible representations for one or the other of the diatomic groups $C_{\infty v}$ and $D_{\infty h}$. $(m_e/2\pi\hbar^2)\langle \mathbf{q}\delta \mid T \mid \mathbf{k}p)$ and $(m_e/2\pi\hbar^2)\langle q\lambda\mu\delta \mid T \mid \mathbf{k}p)$ are scattering amplitudes for the processes

$$X(p\,\mathbf{k}) + Y(p\mathbf{k}) \rightarrow XY^{+}(\delta) + e^{-}(\mathbf{q})$$

and

$$X(p\,\mathbf{k}) + Y(p\mathbf{k}) \rightarrow XY^{+}(\delta) + e^{-}(q\lambda\mu) ,$$

respectively.

With these definitions and notations in hand we now can write cross-section formulas for associative ionization. Our attention will be confined to the integral cross section since this is the observable which has been measured.[1-3] In the case of distinguishable nuclei this cross section is given by the expression

$$\sigma(\hat{\boldsymbol{\alpha}},E) = (m_e/2\pi\hbar^2)^2 \times \sum_{\gamma}\sum_{n,n'}\int d\hat{\mathbf{q}}\int d\mathbf{k}(v_\gamma/v)P(\mathbf{k})P_X(n)P_Y(n') \times \mid\langle \mathbf{q}\gamma \mid T \mid \mathbf{k}nn'\rangle\mid^2 , \tag{2.11}$$

with the γ summation extending over all open channels and with

$$v_\gamma/v = \mu q/m_e k \tag{2.12}$$

equal to the ratio of the speed of the free electron to the relative speed of the two colliding atoms. Formula (2.11), as well as other cross-section formulas in this paper, is also appropriate for cross sections specific to a *narrow range* of q. We only need limit the sum over γ to final states consistent with energy conservation. $P(\mathbf{k})$ is the probability that the initial relative momentum equals $\hbar\mathbf{k}$ and $E = \int d\mathbf{k}P(\mathbf{k})\hbar^2k^2/2\mu$ is the mean of the associated relative kinetic energy. It is assumed that the distribution $P(\mathbf{k})$ is sharply peaked in a direction $\hat{\mathbf{k}}_0$.

By using (2.10) and selecting $\mid\delta\rangle$ to be identical with $\mid\gamma\rangle$, (2.11) can be rewritten in the form

$$\sigma(\hat{\boldsymbol{\alpha}},E) = \sum_{p,p'}\rho_{pp'}(\hat{\boldsymbol{\alpha}})\sigma_{pp'}(E) , \tag{2.13}$$

with

$$\sigma_{pp'}(E) = (m_e/2\pi\hbar^2)^2 \times \sum_{\lambda,\mu}\sum_{\gamma}\int d\mathbf{k}\langle q\lambda\mu\gamma \mid T \mid \mathbf{k}p) \times P(\mathbf{k})(v_\gamma/v)\langle q\lambda\mu\gamma \mid T \mid \mathbf{k}p')^{*} \tag{2.14}$$

and

$$\rho_{pp'}(\alpha) = \sum_{n,n'} P_X(n)P_Y(n')(p \mid nn'\rangle\langle nn' \mid p') . \tag{2.15}$$

The basic formula (2.13) expresses the integral cross section for AI in terms of single-state and interference cross sections, $\sigma_{pp}(E)$ and $\sigma_{pp'}(E)$ with $p\neq p'$, which are specific to the states $\mid p)$ and $\mid p')$ but have no dependence whatsoever on the populations of these states nor the means by which they are populated. In particular, these cross sections are independent of the polarization and intensity of the laser. The dependence of $\sigma(\hat{\boldsymbol{\alpha}},E)$ on the laser intensity is confined to the probabilities $P_X(n)$ and $P_Y(n')$ and the dependence upon $\hat{\boldsymbol{\alpha}}$ is completely incorporated within the factors $(p \mid nn'\rangle$ and $\langle nn' \mid p')$. Thus, the collision dynamics determines the cross sections $\sigma_{pp}(E)$ and $\sigma_{pp'}(E)$, $p\neq p'$, and the laser preparation of the atomic hyperfine states determines the density matrix $\rho_{pp'}(\hat{\boldsymbol{\alpha}})$. Because the elements of the density matrix can be computed analytically (see paper I and Secs. III and IV below), it is clear that measurements of the integral cross section $\sigma(\hat{\boldsymbol{\alpha}},E)$ can be used to gain information about the state-specific cross sections.

The cross-section formulas that we have just presented will now be generalized to include the effects of nuclear statistics. Although these are normally expected to be small, there are situations for which the effects of nuclear indistinguishability can become experimentally observable. The question of concern here is how nuclear indistinguishability affects the polarization dependence of the integral cross section for AI. We shall find [cf. the discussion following (2.24)] that the dependence upon polarization usually is given by the theory for distinguishable nuclei. Numerical estimates of the effects associated with Na-Na collisions are included in Sec. VI. For the AI processes of concern here, these changes turn out to be rather small.

It is necessary at this point to become more explicit about the quantum numbers of the states represented by the kets $\mid\gamma\rangle$ and $\mid p)$. Thus, we write

$$\mid\gamma\rangle = \mid \Lambda_\gamma, Q, B, \nu; \mathscr{S}\Omega_{\mathscr{S}}; \mathscr{I}\Omega_{\mathscr{I}}(II')\rangle , \tag{2.16}$$

with Λ_γ denoting the projection (in units of $\hbar$) of electronic orbital angular momentum along the internuclear axis of the XY^{+} ion. Q is the total orbital angular momentum quantum number of the ion and B is the projection quantum number of this angular momentum on the direction $\hat{\mathbf{k}}$. ν denotes the vibrational quantum number of the ion. $\mathscr{S}$ and $\Omega_{\mathscr{S}}$ are the corresponding pair of electron spin quantum numbers for *all* of the electrons. Finally, I and I' are the spins of the two nuclei, $\mathscr{I}$ is the quantum number of the total nuclear spin, and $\Omega_{\mathscr{I}}$ is the projection quantum number of this total spin on the direction $\hat{\mathbf{k}}$.

The generalization of (2.11) to include nuclear statistics now can be written as[13]

$$\sigma(\hat{\alpha},E)=(m_e/2\pi\hbar^2)^2N \times\sum_{\gamma}\sum_{n,n'}\int d\hat{\mathbf{q}}\int d\mathbf{k}(v_\gamma/v)P(\mathbf{k})P_X(n)P_Y(n') \times|a(\gamma)\langle\mathbf{q}\gamma\mid T\mid\mathbf{k}nn'\rangle +b(\gamma)\langle\mathbf{q}\bar{\gamma}\mid T\mid\mathbf{k}nn'\rangle|^2 \tag{2.17}$$

with $\bar{\gamma}$ denoting the same set of quantum numbers as γ except for Λ_γ, which is replaced with $\bar{\Lambda}_\gamma=-\Lambda_\gamma$. The factor N is defined by

$$N=(1+\Delta)^{-1}, \tag{2.18}$$

with $\Delta=1$ for identical nuclei and $\Delta=0$ otherwise. Finally, the two numbers $a(\gamma)$ and $b(\gamma)$ are given by the formulas

$$a(\gamma)=1+\Delta(-1)^{\mathcal{I}+Q}\delta_{\Lambda_\gamma,0} \tag{2.19}$$

and

$$b(\gamma)=\Delta(-1)^{\mathcal{I}+Q}(1-\delta_{\Lambda_\gamma,0}) . \tag{2.20}$$

The use of (2.10) allows us to obtain an equation for $\sigma(\hat{\alpha},E)$ of the form (2.13), with the same density matrix as before [namely that defined by (2.15)], but with the state-specific cross sections previously defined by (2.14) replaced with those given by the formula

$$\sigma_{pp'}(E)=(m_e/2\pi\hbar^2)^2N\sum_{\lambda,\mu}\sum_{\gamma}\int d\mathbf{k}P(\mathbf{k})(v_\gamma/v)[a(\gamma)\langle q\lambda\mu\gamma\mid T\mid\mathbf{k}p)+b(\gamma)\langle q\lambda\mu\bar{\gamma}\mid T\mid\mathbf{k}p)] \times[a(\gamma)\langle q\lambda\mu\gamma\mid T\mid\mathbf{k}p')+b(\gamma)\langle q\lambda\mu\bar{\gamma}\mid T\mid\mathbf{k}p')]^* . \tag{2.21}$$

In order to convert this expression into a more useful and revealing form we specify that the sets of initial-state quantum numbers p and p' include the *total* nuclear and *total* electron spins as well as the projection quantum numbers of these spins in the direction $\hat{\mathbf{k}}$. Thus, in an obvious notation, p includes $\mathcal{S}_p,\Omega_{\mathcal{S}_p},\mathcal{I}_p$, and $\Omega_{\mathcal{I}_p}$ so that

$$|p)=|x;\mathcal{S}_p\Omega_{\mathcal{S}_p};\mathcal{I}_p\Omega_{\mathcal{I}_p}) . \tag{2.22}$$

The symbol x appearing here denotes the remaining set of "molecular type," initial-state quantum numbers, one of which is $\Lambda_p=\Lambda_x$, the projection of the total electronic orbital angular momentum in the direction $\hat{\mathbf{k}}$.[14] Since the matrix element $\langle q\lambda\mu\gamma\mid T\mid\hat{\mathbf{k}}p)$ is to be computed using a spin-independent Hamiltonian and treating the nuclei as if they were indistinguishable, it can be written in the form

$$\langle q\lambda\mu\gamma\mid T\mid\mathbf{k}p) =\langle q\lambda\mu\mathcal{S}\xi||T||\mathbf{k}\mathcal{S}x)\delta_{\mathcal{S}\mathcal{S}_p}\delta_{\Omega_{\mathcal{S}}\Omega_{\mathcal{S}_p}}\delta_{\mathcal{I}\mathcal{I}_p}\delta_{\Omega_{\mathcal{I}}\Omega_{\mathcal{I}_p}} . \tag{2.23}$$

Here $\langle q\lambda\mu\mathcal{S}\xi||T||\mathbf{k}\mathcal{S}x)$ is a "reduced transition matrix" which depends on $\xi\equiv(\Lambda_\gamma,Q,B,\nu)$ and x rather than upon γ and p.

The result of inserting (2.23) into (2.21) is the formula

$$\sigma(\hat{\alpha},E)=\sum_{x,x'}\sum_{\mathcal{S}}\sigma^{(+)}_{xx'}(\mathcal{S},E)\sum_{\mathcal{I}_e}\rho_{xx'}(\mathcal{I}\mathcal{S},\hat{\alpha}) +\sum_{x,x'}\sum_{\mathcal{S}}\sigma^{(-)}_{xx'}(\mathcal{S},E)\sum_{\mathcal{I}_o}\rho_{xx'}(\mathcal{I}\mathcal{S},\hat{\alpha}) , \tag{2.24}$$

with $\mathcal{I}_e$ denoting the set of all even values of $\mathcal{I}$ and $\mathcal{I}_o$ the set of all odd $\mathcal{I}$. The density matrix appearing in this expression is defined by

$$\rho_{xx'}(\mathcal{I}\mathcal{S},\hat{\alpha}) =\sum_{\Omega_{\mathcal{S}},\Omega_{\mathcal{I}}}\sum_{n,n'}P_X(n)P_Y(n') \times(x;\mathcal{S}\Omega_{\mathcal{S}}\mathcal{I}\Omega_{\mathcal{I}}\mid nn') \times\langle nn'\mid x';\mathcal{S}\Omega_{\mathcal{S}}\mathcal{I}\Omega_{\mathcal{I}}) \tag{2.25}$$

and the cross sections by

$$\sigma^{(\pm)}_{xx'}(\mathcal{S},E)=N(m_e/2\pi\hbar^2)^2\sum_{\lambda,\mu}\sum_{\xi}\int d\mathbf{k}P(\mathbf{k})(v_\xi/v) \times\{[1+(1+2p^{\pm})\Delta\delta_{\Lambda_\xi,0}]\langle q\lambda\mu\mathcal{S}\xi||T||\mathbf{k}\mathcal{S}x)\langle q\lambda\mu\mathcal{S}\xi||T||\mathbf{k}\mathcal{S}x')^* +[p^{\pm}(1-\delta_{\Lambda_\xi,0})\Delta][\langle q\lambda\mu\mathcal{S}\xi||T||\mathbf{k}\mathcal{S}x)\langle q\lambda\mu\mathcal{S}\bar{\xi}||T||\mathbf{k}\mathcal{S}x')^* +\langle q\lambda\mu\mathcal{S}\bar{\xi}||T||\mathbf{k}\mathcal{S}x)\langle q\lambda\mu\mathcal{S}\xi||T||\mathbf{k}\mathcal{S}x')^*] +[(1-\delta_{\Lambda_\xi,0})\Delta]\langle q\lambda\mu\mathcal{S}\bar{\xi}||T||\mathbf{k}\mathcal{S}x)\langle q\lambda\mu\mathcal{S}\bar{\xi}||T||\mathbf{k}\mathcal{S}x')^*\} . \tag{2.26}$$

In the second of these formulas $v_{\xi}=v_{\gamma}$, $\Lambda_{\xi}=\Lambda_{\gamma}$, and

$$p^{\pm}=(-1)^{2I+(1/2)\mp(1/2)+Q} . \tag{2.27}$$

The set $\bar{\xi}$ is the same as $\xi=(\Lambda_{\xi},Q,B,\nu)$ except that Λ_{ξ} is replaced with $\bar{\Lambda}_{\xi}=-\Lambda_{\xi}$.

The formulas for the AI integral cross section provided by equations (2.24)—(2.26) are quite general and, as such, deserve several comments. The first of these concerns distinguishable nuclei, in which case $\Delta=0$. From (2.26) it then follows that $\sigma_{xx'}^{(+)}$ and $\sigma_{xx'}^{(-)}$ have a common value, $\sigma_{xx'}$, so that (2.24) reduces to the familiar form [see (2.13)—(2.15)]

$$\sigma(\hat{\boldsymbol{\alpha}},E)=\sum_{x,x'}\sum_{\mathscr{S}}\sigma_{xx'}(\mathscr{S},E)\sum_{\mathscr{I}}\rho_{xx'}(\mathscr{I}\mathscr{S},\hat{\boldsymbol{\alpha}}) . \tag{2.28}$$

A second observation hinges upon the fact that the algebraic sign of $p^{\pm}$ changes with each successive value of the orbital angular momentum quantum number Q. Therefore, $\sigma_{xx'}^{(+)}$ and $\sigma_{xx'}^{(-)}$ should be approximately equal to one another provided that the objects $\langle q\lambda\mu\mathscr{S}\xi||T||\mathbf{k}\mathscr{S}x\rangle$ $\langle q\lambda\mu\mathscr{S}\xi'||T||\hat{\mathbf{k}}\mathscr{S}x'\rangle^{*}$ are slowly varying functions of Q over the allowed range of this quantum number. $\sigma_{xx'}^{(+)}$ and $\sigma_{xx'}^{(-)}$ may, of course, be different if only a few values of Q contribute to the rate of reaction. It is precisely when this happens that one can expect to see significant effects due to nuclear statistics. For example, in AI few if any Q values will be open to reaction when the measurements are restricted to an electron-energy differential cross section and the initial velocity distribution $P(\mathbf{k})$ is sufficiently narrow. $\sigma_{xx'}^{(+)}$ and $\sigma_{xx'}^{(-)}$ may also differ from one another in the vicinity of a channel threshold. Furthermore, small values of the initial relative kinetic energy and/or processes involving light nuclei will limit the set of participating Q's, and so may produce observable consequences of nuclear statistics. It is worthy of notice that even though $\sigma_{xx'}^{(+)}$ and $\sigma_{xx'}^{(-)}$ may be nearly equal, they are specific to different processes. For example, in the case of $\Lambda_{\xi}=0$ (the XY^{+} product ion in a Σ state) $\sigma_{xx'}^{(+)}$ is a cross section for the production of ions with even values of $2I+Q$ whereas $\sigma_{xx'}^{(-)}$ pertains to ions with odd values of $2I+Q$. This is related to the absence of states with odd values of $2I+Q+\mathscr{I}$ from the spectra of diatomic molecules with indistinguishable nuclei. Finally, it is clear from (2.24) that, all other considerations aside, nuclear statistics will have little effect upon the polarization dependence of the AI integral cross section when $\sum_{\mathscr{I}_o}\rho_{xx'}(\mathscr{I}\mathscr{S},\hat{\boldsymbol{\alpha}})$ and $\sum_{\mathscr{I}_e}\rho_{xx'}(\mathscr{I}\mathscr{S},\hat{\boldsymbol{\alpha}})$ are nearly equal. This often is the case (cf. Sec. VI).

C. Selection rules

We have stated repeatedly that formulas such as (2.13) and (2.24) can be used in conjunction with experimental measurements of the AI cross section $\sigma(\hat{\boldsymbol{\alpha}},E)$ to obtain information about the state-specific cross sections $\sigma_{pp'}(E)$ and/or $\sigma_{xx'}^{(\pm)}(\mathscr{S},E)$. The efficacy of this procedure will be enhanced if we can succeed in establishing that some of the $\sigma_{xx'}^{(\pm)}$ are equal to zero or are, at least, very nearly so. This objective can be achieved by invoking a number of selection rules. Detailed proofs of these rules are not presented here but can be found in Refs. 4 and 11.

It will be recalled that $\langle q\lambda\mu\mathscr{S}\xi||T||\mathbf{k}\mathscr{S}x\rangle$ is computed as if the nuclei were distinguishable. Therefore, we elect to associate nucleus A with atom X and nucleus B with atom Y. Furthermore, the set x includes Λ_x, the projection quantum number of the electronic orbital angular momentum along $\hat{\mathbf{k}}$. We now observe that prior to collision the direction of the internuclear vector, $\mathbf{R}=\mathbf{R}_B-\mathbf{R}_A$, coincides with that of the initial relative momentum $\mathbf{k}$. Consequently, the precollisional value of the projection along $\hat{\mathbf{k}}$ of the *total* orbital angular momentum is equal to $\hbar\Lambda_x$. The postcollisional value of this same component of the total orbital angular momentum is $\hbar(\mu+B)$. Since the collision dynamics are governed by a spin-free Hamiltonian the total orbital angular momentum is a constant of the motion and

$$\langle q\lambda\mu\mathscr{S}\xi||T||\mathbf{k}\mathscr{S}x\rangle\propto\delta_{\mu+B,\Lambda_x} . \tag{2.29}$$

The result of inserting this into (2.26) is the selection rule

$$\sigma_{xx'}^{(\pm)}(\mathscr{S},E)\propto\delta_{\Lambda_x,\Lambda_{x'}} . \tag{2.30}$$

If the two nuclei have the same atomic number, then both of the sets x and ξ will include total electronic parity quantum numbers. Let us denote the initial-state parity by π_x and the parity of the XY^{+} ion by π_{ξ}. The parity of the final state $|\,q\lambda\mu\mathscr{S}\xi\rangle$ is then $\pi_{\xi}(-1)^{\lambda}$. The conservation of total electronic parity implies that

$$\langle q\lambda\mu\mathscr{S}\xi||T||\mathbf{k}\mathscr{S}x\rangle\propto\delta_{\pi_{\xi}(-1)^{\lambda},\pi_x} \tag{2.31}$$

and this, when combined with (2.26), produces the selection rule

$$\sigma_{xx'}^{(\pm)}(\mathscr{S},E)\propto\delta_{\pi_x,\pi_{x'}} . \tag{2.32}$$

The composite statement of the selection rules (2.23), (2.30), and (2.32) is that the interference cross section connecting two sets of initial-state quantum numbers p and p' can be different from zero only if $\mathscr{I}_p=\mathscr{I}_{p'}$, $\Omega_{\mathscr{I}p}=\Omega_{\mathscr{I}p'}$, $\mathscr{S}_p=\mathscr{S}_{p'}$, $\Omega_{\mathscr{S}p}=\Omega_{\mathscr{S}p'}$, $\Lambda_p=\Lambda_{p'}$, and $\pi_p=\pi_{p'}$. The sole limitation upon the validity of these selection rules is the assumption that the collision dynamics are governed by a Hamiltonian operator which is devoid of spin-orbit couplings.

These considerations permit one to draw firm conclusions about the interference cross sections associated with the quasimolecular basis. However, even if all of these were to vanish, the interference terms associated with a different initial-state basis would not, in general, be equal to zero. To be more specific let us transform (2.13) from the quasimolecular basis to another, the states of which are labeled with Latin indices. The integral cross section then can be rewritten in the form

$$\begin{aligned}\sigma(\hat{\boldsymbol{\alpha}},E)&=\sum_{p,p'}\rho_{pp'}(\hat{\boldsymbol{\alpha}})\sigma_{pp'}(E)\\&=\sum_{p,p'}\rho_{pp'}(\hat{\boldsymbol{\alpha}})\sum_{i,i'}c_{pi}^{*}c_{p'i'}\sigma_{ii'}(E) ,\end{aligned} \tag{2.33}$$

with c_{pi} denoting a matrix element of the unitary transformation defined by the connection

$$|i)=\sum_p |p)c_{pi} \ . \tag{2.34}$$

Suppose now we somehow have established that $\sigma_{pp'}=\sigma_{pp}\delta_{pp'}$ for all of the quasimolecular states which conceivably could contribute to the observed cross section $\sigma(\hat{\alpha},E)$. (An obvious example is a situation where only one quasimolecular channel is open.) As a consequence of this, (2.33) reduces to

$$\begin{aligned}\sigma(\hat{\alpha},E)&=\sum_p \rho_{pp}(\hat{\alpha})\sigma_{pp}(E)\\&=\sum_p \rho_{pp}(\hat{\alpha})\sum_{i,i'} c^*_{pi}c_{pi'}\sigma_{ii'}(E) \ .\end{aligned} \tag{2.35}$$

This identity is valid for any set of states p that includes all reactive states. We now test the *assumption* that $\sigma_{ii'}(E)=\sigma_{ii}(E)\delta_{ii'}$. *If* it is valid, (2.35) then can be rewritten in a form

$$\begin{aligned}\sigma(\hat{\alpha},E)&=\sum_p \rho_{pp}(\hat{\alpha})\sum_i |c_{pi}|^2\sigma_{ii}(E)\\&=\sum_p \rho_{pp}(\hat{\alpha})\sum_i |c_{pi}|^2\sum_{q,q'} c^*_{qi}c_{q'i}\sigma_{qq'}(E)\\&=\sum_p \rho_{pp}(\hat{\alpha})\sum_q \left[\sum_i |c_{pi}|^2|c_{qi}|^2\right]\sigma_{qq}(E) \ ,\end{aligned} \tag{2.36}$$

which must be equivalent to (2.35). This means that the relationship

$$\sum_p \rho_{pp}(\hat{\alpha})\left[\sum_i |c_{pi}|^2|c_{qi}|^2\right]-\rho_{qq}(\hat{\alpha})=0 \tag{2.37}$$

must be satisfied for all states such that $\sigma_{qq}(E)\neq 0$, and for any set of states p that includes all reactive quasimolecular states. From this, we also find

$$\rho_{pp}\left[\sum_i |c_{pi}|^2|c_{qi}|^2\right]=0 \tag{2.37'}$$

must be satisfied for any reactive q and nonreactive p.

Equations (2.37) and (2.37') often are *not* satisfied. At least in these cases, the resulting conclusion is that $\sigma(\hat{\alpha},E)$ cannot be represented in the form $\sigma(\hat{\alpha},E)=\sum_i \rho_{ii}(\hat{\alpha})\sigma_{ii}(E)$. Whether this form is numerically accurate in a particular instance may be discovered by checking the magnitude of any interference terms, but it cannot simply be assumed. Examples where (2.37) and (2.37') are violated easily can be found. For example, if only one q is reactive, (2.37') is clearly violated since $\sum_i |c_{qi}|^2|c_{qi}|^2$ will not be unity [unless $|q)$ is identical to some $|i)$]. Another example results when the states $|q)$ and $|i)$ both include the quantum number Ω, specifying the projection of total angular momentum on the laboratory z axis. One then can verify that (2.37') is violated under the experimental conditions studied in Sec. VI, if $|i)$ is a direct product of atomic states, labeled by quantum numbers such as (L,M_L,S,M_S) (Ref. 8) or (L,S,J,M_J).[1,9] Since the integral cross section for this process is of the form (1.2) [or (2.35)], the above comments regarding $\sigma(\hat{\alpha},E)=\sum_i \rho_{ii}(\hat{\alpha})\sigma_{ii}(E)$ apply fully.

This illustrates the danger of a cavalier disregard for the contributions of interference cross sections. An analysis that disregarded this fact could yield invalid conclusions. If it appears that we are unduly stressing the rather obvious fact that a matrix known to be diagonal in one representation need not be diagonal in another, it is because arguments to the contrary have received wide currency.

We now derive a more specific selection rule which will be used in Sec. VI. It is assumed that the initial electronic state is a Σ state ($\Lambda_p=\Lambda_x=0$). The quantum number associated with the reflection of this state in a plane containing the internuclear axis $\mathbf{R}$ is denoted by σ_x. The state of the product XY^+ ion also is taken to be a Σ state ($\Lambda_\gamma=\Lambda_\xi=0$) with a reflection quantum number σ_ξ. There is an approximate selection rule specific to this case,[12] according to which the projection along $\mathbf{R}$ of the free-electron's orbital angular momentum is zero. Consequently, the reflection quantum number of the free-electron orbital will equal unity and this, in turn, means that the reflection quantum number of the ket $|q\lambda\mu\xi\mathcal{S})$ is σ_ξ. Because the reflection character of the electronic states is a collisional invariant, it then follows that

$$\langle q\lambda\mu\mathcal{S}\xi||T||\mathbf{k}\mathcal{S}x)\propto\delta_{\sigma_\xi,\sigma_x} \quad \text{for } \Lambda_x=\Lambda_\xi=0 \ . \tag{2.38}$$

According to this, a collision beginning in a quasimolecular Σ^- state cannot result in a product Σ^+ diatomic ion.

The selection rule used in deriving (2.38) is obtained by treating the component of electronic orbital angular momentum along the internuclear axis as if it were a constant of the motion. This is an approximation because the axial symmetry of the system is broken by the Coriolis force (rotational Born-Oppenheimer couplings). Nevertheless, it is to be expected that violations of the selection rule (2.38) rarely will occur unless the collision velocity is very large.

Finally, we observe that for relatively small values of the initial-state de Broglie wavelength [e.g., $\lambda_{\text{deB}}\equiv 2\pi/k=2\pi\hbar(2\mu E)^{-1/2}<\frac{1}{2}$ (Bohr radius)] the magnitude of $\sigma^{(\pm)}_{xx'}(\mathcal{S},E)$ will be negligible unless the classical turning point associated with x (for all x') lies within the electronic continuum region of XY^++e^- (cf. Fig. 3). This approximate selection rule is based on arguments involving the overlap of nuclear wave functions and has been discussed elsewhere.[4]

III. DIAGRAMMATIC METHODS FOR ANGULAR MOMENTUM ALGEBRA

In Sec. IV we shall obtain an explicit formula for the density matrix $\rho_{xx'}(\mathcal{I}\mathcal{S},\hat{\alpha})$ defined by (2.25). As already pointed out in Sec. II, this will establish a linear algebraic connection (cf. 2.24) between the experimentally determined integral cross section for AI and the single-state and interference cross sections, $\sigma^{(\pm)}_{xx}$ and $\sigma^{(\pm)}_{xx'}$ ($x\neq x'$), respectively. The process of evaluating the density matrix is a tedious exercise in angular momentum algebra which can be expedited by the introduction of diagrammatic

techniques.[15] The diagrammatic and algebraic methods are, of course, equivalent, the principle advantage of the former being that one can invoke geometric intuition to simplify complicated algebraic expressions. Since these techniques are useful, but probably unfamiliar to most readers, we provide here a resumé tailored to the needs of Sec. IV.

A. Angular momentum eigenstates

The angular momentum eigenket associated with a generic angular momentum $\mathbf{j}$ is so defined that

$$\begin{aligned} \mathbf{j}^2 \mid jm\rangle &= \hbar^2 j(j+1) \mid jm\rangle \ , \\ j_z \mid jm\rangle &= \hbar m \mid jm\rangle \ . \end{aligned} \tag{3.1}$$

We adopt the usual phase convention[15,16] for these and all other angular momentum kets, namely, that

$$(j_x \pm i j_y) \mid jm\rangle = \hbar[(j \mp m)(j \pm m+1)]^{1/2} \mid j, m \pm 1\rangle \ . \tag{3.1'}$$

Beginning with n commuting angular momenta $\mathbf{j}_\alpha$ ($\alpha = 1, \ldots, n$), we can establish a coupling scheme which incorporates a number of "intermediate" angular momentum l_β. Each of these intermediate angular momenta is the sum of two other angular momenta, either or both of which also *may* be intermediates. Only one rule need be observed in constructing the coupling scheme, namely, that once any angular momentum one $\mathbf{j}_\alpha$ (l_β) appears, it can occur in the definition of only (one other) intermediate angular momentum. It is possible to define $n-1$ intermediates, l_β, including

$$\mathbf{g} \equiv \boldsymbol{l}_{n-1} \equiv \sum_{\alpha=1}^{n} \mathbf{j}_\alpha \ . \tag{3.2}$$

We soon shall construct simultaneous eigenkets of $\mathbf{j}_\alpha^2$ ($\alpha = 1, \ldots, n$), $\boldsymbol{l}_\beta^2$ ($\beta = 1, \ldots, n-1$), and $l_{n-1,z} \equiv \mathbf{g}_z$ and then adopt one of two notations for these states. Thus, if there is no cause for confusion (the coupling scheme is known and fixed) we shall denote the quantum numbers associated with the set $\boldsymbol{l}_\beta^2$ ($\beta = 1, \ldots, n-2$) by the letter a, the quantum numbers associated with the set $\mathbf{j}_\alpha^2$ ($\alpha = 1, \ldots, n$) by $\{j\}$, and the quantum numbers for $\mathbf{g}^2$ and g_z by g and m_g, respectively. The simultaneous eigenket of all these operators is then denoted by the symbol $\mid \{j\} a g m_g\rangle$. It satisfies the equations

$$\begin{aligned} \mathbf{j}_\alpha^2 \mid \{j\} a g m_g\rangle &= \hbar^2 j_\alpha(j_\alpha+1) \mid \{j\} a g m_g\rangle \ , \qquad \alpha = 1, \ldots, n \\ \boldsymbol{l}_\beta^2 \mid \{j\} a g m_g\rangle &= \hbar^2 l_\beta(l_\beta+1) \mid \{j\} a g m_g\rangle \ , \qquad \beta = 1, \ldots, n-2 \\ \mathbf{g}^2 \mid \{j\} a g m_g\rangle &= \hbar^2 g(g+1) \mid \{j\} a g m_g\rangle \\ g_z \mid \{j\} a g m_g\rangle &= \hbar m_g \mid \{j\} a g m_g\rangle \ . \end{aligned} \tag{3.3}$$

On the other hand, when it is necessary to indicate the coupling scheme, we shall do so by using a nested set of parentheses. For example, the symbol $(j_1, j_2) l_1$, containing the quantum number j_1, j_2, and l_1 (corresponding to the three angular momenta $\mathbf{j}_1$, $\mathbf{j}_2$, and $\boldsymbol{l}_1$, respectively), indicates that $\mathbf{j}_1 + \mathbf{j}_2 = \boldsymbol{l}_1$. Similarly, the symbol

$$((j_1, j_2) l_1, (j_3, j_4) l_2) g$$

indicates that $\mathbf{j}_1 + \mathbf{j}_2 = \boldsymbol{l}_1$, $\mathbf{j}_3 + \mathbf{j}_4 = \boldsymbol{l}_2$, and $\mathbf{l}_1 + \mathbf{l}_2 = \mathbf{g} \equiv \boldsymbol{l}_3$.

B. Addition of angular momentum

Consider two angular momentum kets $\mid \xi JM\rangle$ and $\mid \zeta KM\rangle$, the first of which is an eigenstate of $\mathbf{J}^2$ and J_z with corresponding quantum numbers J and M and the second of which is an eigenstate of $\mathbf{K}^2$ and K_z with quantum numbers K and N. The letters ξ and ζ denote additional quantum numbers not related to $\mathbf{J}$ and $\mathbf{K}$. If $\mathbf{J}$ and $\mathbf{K}$ commute, we can immediately construct the object

$$\mid \xi\zeta(JK) L M_L\rangle = \sum_{M,N} \mid \xi JM\rangle \mid \zeta KN\rangle \langle JMKN \mid LM_L\rangle \ , \tag{3.4}$$

which is an eigenket of each of the operators $\mathbf{J}^2$, $\mathbf{K}^2$, $\mathbf{L}^2$ ($\mathbf{L} = \mathbf{J} + \mathbf{K}$), and L_z with eigenvalues $\hbar^2 J(J+1)$, $\hbar^2 K(K+1)$, $\hbar^2 L(L+1)$, and $\hbar M_L$, respectively. The ket defined by (3.4) is, as well, an eigenstate of the operators associated with the quantum numbers ξ and ζ

The symbol $\langle JMKN \mid LM_L\rangle$ is the usual Clebsch-Gordon coefficient. For future reference we recall the following basic properties of these coefficients:

$$\langle a\alpha b\beta \mid c\gamma\rangle = [c]^{1/2}(-1)^{a-b+\gamma} \begin{pmatrix} a & b & c \\ \alpha & \beta & -\gamma \end{pmatrix} , \tag{3.5}$$

with $[x] \equiv 2x+1$ and where $\left(\begin{smallmatrix} Q & R & S \\ q & r & s \end{smallmatrix}\right)$ is the $3j$ symbol;

$$\delta_{cc'}\delta_{\gamma\gamma'} = \sum_{\alpha,\beta} \langle c\gamma \mid a\alpha b\beta\rangle \langle a\alpha b\beta \mid c'\gamma'\rangle \ , \tag{3.6}$$

$$\delta_{\alpha\alpha'}\delta_{\beta\beta'} = \sum_{c,\gamma} \langle a\alpha b\beta \mid c\gamma\rangle \langle c\gamma \mid a\alpha' b\beta'\rangle \ , \tag{3.7}$$

and the coefficients are real, i.e.,

$$\langle a\alpha b\beta \mid c\gamma\rangle = \langle c\gamma \mid a\alpha b\beta\rangle \ . \tag{3.8}$$

From the discussion of Sec. III A it follows that whenever we wish to introduce a new intermediate angular momentum, we add two commuting angular momenta. Thus, by repeated applications of (3.4) we can generate $\mid \{j\} a g m_g\rangle$ from the product states $\mid j_1 m_1\rangle \cdots \mid j_n m_n\rangle \equiv \mid \{m\}\rangle$. This is denoted as follows:

$$\mid \{j\} a g m_g\rangle = \sum_{\{m\}} \langle \{m\} \mid \{j\} a g m_g\rangle \mid \{m\}\rangle \ . \tag{3.9}$$

It is straightforward to show [using (3.6) and (3.7)] that the transformation (3.9) is unitary, i.e., that

$$\delta(\{m\}, \{m'\}) = \sum_{a,g,m_g} \langle \{m\} \mid \{j\} a g m_g\rangle \langle \{j\} a g m_g \mid \{m'\}\rangle \tag{3.10}$$

and

$$\delta_{aa'}\delta_{gg'}\delta_{m_g m_g'} = \sum_{\{m\}} \langle \{j\} a g m_g \mid \{m\}\rangle \langle \{m\} \mid \{j\} a' g' m_g'\rangle \ . \tag{3.11}$$

The real-valued objects $\langle \{j\} a g m_g \mid \{m\}\rangle$ are called *gen-*

eralized Clebsch-Gordon coefficients (GCGC). They play an important role in what follows.

C. The transformation matrix

The problem encountered in this section is closely related to that of evaluating the inner product of two angular momentum eigenkets $|u\rangle$ and $|v\rangle$. These may be individual kets of the type $|\{j\}agm_g\rangle$ or direct products $|\{j^1\}a^1g^1m_g^1\rangle\cdots|\{j^p\}a^pg^pm_g^p\rangle$ formed from disjoint sets of angular momenta, $\{j_\alpha^i\}$ with $i=1,\ldots,p$ and $\alpha=1,\ldots,n_i$. We impose the obvious restriction that $|u\rangle$ and $|v\rangle$ be eigenkets associated with a common set of angular momenta. Then, with $|\{\{m\}\}\rangle$ denoting the direct product of all the kets $|j_\alpha^i m_\alpha^i\rangle$ belonging to this set, it follows that

$$\langle u|v\rangle=\sum_{m_\alpha^p}\langle u|\{\{m\}\}\rangle\langle\{\{m\}\}|v\rangle\ . \tag{3.12}$$

The objects $\langle u|v\rangle$ are elements of the *transformation matrix*, so called because it connects states having different coupling schemes. The form of the right-hand side of (3.12) demonstrates that an element of the transformation matrix can be expressed as a sum of products of GCGC's. This observation will be useful when we reach the stage of constructing diagrammatic representations of $\langle u|v\rangle$ and similar objects.

D. Graphical representations of algebraic expressions

We are now ready to introduce graphical representations of the algebraic objects discussed in the preceding parts of this section. Once the transcription into this representation has been made we can concentrate on the manipulation (simplification) of diagrams, a task considered in Sec. III E.

There are two "fundamental" diagrams; all others are constructed from these. One is the diagram for the $3j$ symbol, $\begin{pmatrix} a & b & c \\ \alpha & \beta & \gamma \end{pmatrix}$,

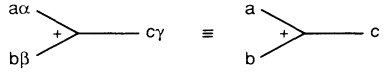

(3.13)

The plus sign attached to this graph indicates that the motion in going from $(a\alpha)\rightarrow(b\beta)\rightarrow(c\gamma)$ is counterclockwise. By using the symmetry properties of the $3j$ symbols one can show that the object represented by this diagram is unchanged by a cyclic permutation of the lines labeled a, b, and c. As indicated by the figure, the magnetic quantum numbers α, β, and γ are suppressed whenever their omission produces no confusion. We also define another symbol equivalent to $\begin{pmatrix} a & b & c \\ \alpha & \beta & \gamma \end{pmatrix}$,

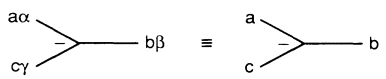

(3.14)

The minus sign appearing here indicates the motion associated with the sequence $(a\alpha)\rightarrow(b\beta)\rightarrow(c\gamma)$ is in the clockwise direction. This symbol also is invariant with respect to cyclic permutations of the line segments.

The preceding considerations, taken together with the familiar symmetries of the $3j$ symbols, show that the algebraic meaning of a $3j$ diagram is unchanged when we (1) permute two lines and change the sign of the diagram, (2) change the sign of the diagram and multiply the result with $(-1)^{a+b+c}$, and (3) permute two lines and multiply with $(-1)^{a+b+c}$.

The second fundamental diagram corresponds to the so-called "metric tensor"

$$\begin{bmatrix} a \\ \alpha\alpha' \end{bmatrix}\equiv(-1)^{a+\alpha}\delta_{\alpha,-\alpha'}\ , \tag{3.15}$$

The diagram for this object is

(3.16)

We now consider an expression of the form

$$\underline{B}=\sum_{\text{all }\gamma}\underline{F}(Q;_\gamma^c)\underline{G}(R;_\gamma^c)\underline{H}(S)\ , \tag{3.17}$$

with $\underline{F}$ and $\underline{G}$ denoting $3j$ symbols or metric tensors and $\underline{H}$ a sum of products of $3j$ symbols and metric tensors. Q, R, and S are angular momentum quantum numbers other than c and γ. Any summed magnetic quantum number, such as γ in (3.17), is called "contracted." The diagrammatic convention for indicating that γ is contracted is to connect the two $c\gamma$ lines of the diagrams for $\underline{F}$ and $\underline{G}$. This process is repeated for each contracted quantum number in $\underline{B}$. Thus, the diagram for $\underline{B}$ will contain one "node" [±>—] for each $3j$ symbol and, in general, lines connecting the nodes. Some or all of these lines will be decorated with one or more arrows [—►]. We distinguish between "internal lines" which connect two nodes and "external lines" which connect to only one.

Many diagrams are equivalent in the sense that they have identical algebraic meanings. To see if two diagrams are equivalent, we first determine whether they are "similar." By definition, two diagrams 1 and 2 are similar if (1) we can deform the lines and nodes of 2 so it lies in coincidence with 1 without breaking any lines; (2) the total angular momentum quantum numbers of corresponding internal lines are then the same, and (3) the total and projection angular momentum quantum numbers of corresponding external lines also are the same. The arrows and signs of nodes are disregarded in performing these steps. Let us call the two nodes in the ith corresponding pair above i_1 and i_2 (it is evident two similar diagrams must have the same number of nodes).

Two similar diagrams also may be equivalent. This requires that (1) the $3j$ symbols associated with i_1 and i_2 (in their original forms) be the same and (2) the arrows on each pair of corresponding lines must be such that the metrics or products of metrics associated with the two are equal.

We soon shall want to replace a diagram with one to which it is equivalent. Equation (3.18) provides a list of identities which can be used for this purpose. Each is readily proved. The validity of these identities is, of course, unaffected by the relationship of the displayed elements to the rest of the diagram.

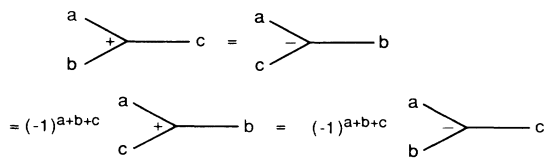

(3.18a)

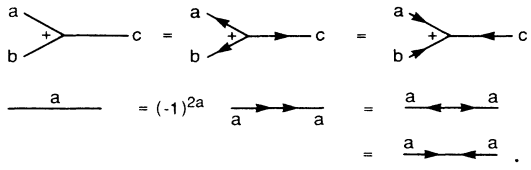

(3.18b)

(3.18c)

To the identities listed here one may add results obtained by cyclic permutation. Any of these may be freely used to convert a diagram into a simpler form—as long as no lines are broken in the process. Some example of this will be given in the paragraphs which follow below.

Our objective is the evaluation of expressions containing matrix elements such as $\langle u \mid v \rangle$ of (3.12). The diagrams for these objects are easy to draw once we know those for Clebsch-Gordon coefficients and GCGC's. We consider these now. From the definition (3.5) and the diagrams already encountered in Sec. III D one finds that the diagram for the Clebsch-Gordon coefficient $\langle a\alpha b\beta \mid c\gamma \rangle$ is

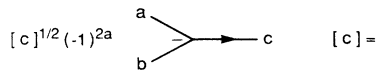

(3.19)

Given this and the preceding discussion, diagrams for the GCGC's can be drawn immediately. One simple draws a Clebesch-Gordon coefficient of the type

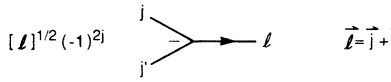

(3.20)

for each intermediate angular momentum $l=\mathbf{j}+\mathbf{j}'$, including $\mathbf{g}$. There will be two lines for every intermediate angular momentum except $\mathbf{g}$. By connecting these pairs one obtains the diagram for the GCGC. All GCGC diagrams have a branch structure (without closed loops) consisting of $n-1$ nodes. The diagram for $\langle u \mid v \rangle$ is obtained by putting several GCGC's together and connecting each pair of j^i_α lines (for all j^i_α).

This is illustrated by constructing the diagram for

$$\langle u \mid v \rangle = \langle ((j_1,j_2)j_{12},(j_3,j_4)j_{34})gm \mid ((j_1,j_3)j_{13},(j_2,j_4)j_{24})g'm' \rangle \ . \tag{3.21}$$

The two GCGC's required for this are

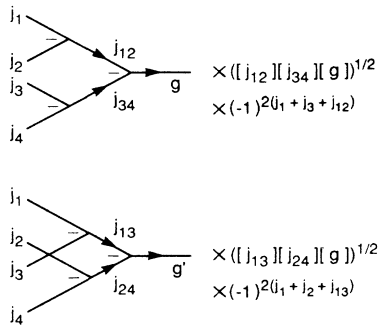

(3.22)

Using (3.12) we then obtain the diagram

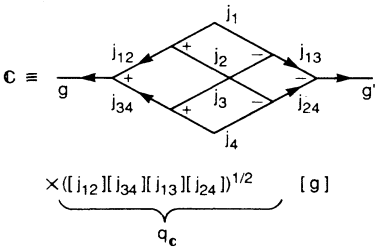

(3.23)

[with $q_c=([j_{12}][j_{34}][j_{13}][j_{24}])^{1/2}$] which is equivalent to $\langle u \mid v \rangle$ defined by (3.21).

E. Simplification of diagrams

Because most diagrams are too complicated for direct numerical evaluation, a procedure is needed for reducing diagrams to sums of readily computed objects, such as $6j$ and $9j$ symbols. The reduction procedure consists of two steps. One first manipulates the diagram into "standard form," namely, a form with *one* arrow on each internal line. This can always be done for the diagrams of GCGC's and for transformation matrix elements $\langle u \mid v \rangle$. The second step is to simplify the standard diagram by a procedure which will now be described.

The main tool used to simplify standard diagrams is the "expansion theorem." Consider a standard graph with N external lines, each without an arrow. (This restriction causes no practical problems.) If we represent this object by the symbol

$$\underline{F}\begin{bmatrix} J_1 & \cdots & J_N \\ M_1 & \cdots & M_N \end{bmatrix} ,$$

then the expansion theorem states that (see Appendix A)

$$\underline{F}\begin{bmatrix} J_1 & \cdots & J_N \\ M_1 & \cdots & M_N \end{bmatrix} = (-1)^{J_N - M_N} \sum_a R(a) \langle \{J\} a J_N - M_N \mid \{M\} \rangle \ , \tag{3.24}$$

with

$$R(a) = [J_N]^{-1} \sum_{\{M'\}} \sum_q \underline{F}\begin{bmatrix} J_1 & \cdots & J_N \\ M'_N & & M'_N \end{bmatrix} \times \begin{bmatrix} J_N \\ qM'_N \end{bmatrix} \langle \{J\} a J_N q \mid \{M'\} \rangle \ , \tag{3.25}$$

and where $\{J\} \equiv J_1, \ldots, J_{N-1}$, $\{M\} \equiv M_1, \ldots, M_{N-1}$, and $\{M'_N\} \equiv M', \ldots, M'_{N-1}$. $\langle \{J\} a J_N q \mid \{M'\} \rangle$ is the previously defined GCGC. This expansion theorem applies even for $N=1$ and 2 provided that we delete the sum over a and define

$$\langle\{J\}aJ_2M_2\,|\,\{M\}\rangle = \begin{pmatrix} J_1 & J_2 & 0 \\ M_1 & -M_2 & 0 \end{pmatrix}(-1)^{J_1-M_1}[J_2]^{1/2}\delta_{J_1,J_2}\delta_{M_1,-M_2} \tag{3.26}$$

and

$$\langle\{J\}aJ_1M_1\,|\,\{M\}\rangle = \begin{pmatrix} J_1 & 0 & 0 \\ M_1 & 0 & 0 \end{pmatrix} = \delta_{J_1,0}\delta_{M_1,0}\,. \tag{3.27}$$

The formulas (3.24) and (3.25) also apply if

$$\underline{F}\begin{pmatrix} J_1 & \cdots & J_N \\ M_1 & \cdots & M_N \end{pmatrix}$$

is part of a larger diagram. This results in a compelling diagrammatic interpretation of these equations, which is shown below for $N=1$, 2, and 3,

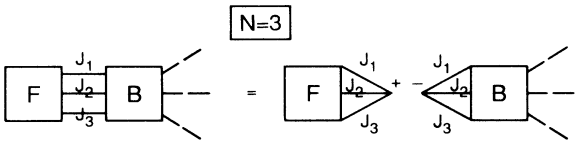

(3.28a)

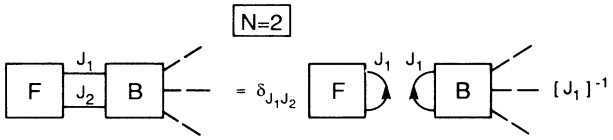

(3.28b)

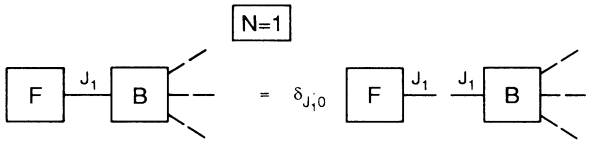

(3.28c)

The square labeled F is a schematic diagram for

$$\underline{F}\begin{pmatrix} J_1 & \cdots & J_N \\ M_1 & \cdots & M_N \end{pmatrix}.$$

B is unrestricted; it may have external lines other than $J_1,\ldots,J_N$ and it need not be in standard form. (Any arrows on $J_1,\ldots,J_N$ can be absorbed into B.) Diagrams that can be changed using figures such as these are called "separable;" they can be separated into products of simple diagrams.

A simple example may prove helpful. Using (3.18) we convert C of (3.23) into standard form:

$$\mathbf{c} = \quad \times(-1)^{2g}\quad q_{\mathbf{c}}\,[g]\,. \tag{3.29}$$

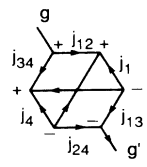

Next we use (3.28b), identifying B with the "unit object" through which the external lines from F pass unaltered. The hexagonal diagram which appears in the result

$$\mathbf{c} = \quad \times\,\delta(gg')\;\delta(m_g m_{g'})\;q_{\mathbf{c}} \tag{3.30}$$

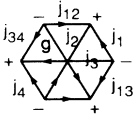

is the $9j$ symbol

$$\begin{Bmatrix} j_4 & j_2 & j_{12} \\ j_3 & j_1 & j_{13} \\ j_{34} & j_{12} & j \end{Bmatrix}.$$

Yutsis, Levinson, and Varagas[15] give a rather complete list of angular momentum identities and so we shall belabor the point no further.

Much of the utility of the diagrammatic method flows from the ease with which (3.28) can be applied. It is easy to look at a diagram and see how it might be simplified. The corresponding algebraic manipulations are invariably more difficult.

IV. DENSITY-MATRIX CALCULATION

The techniques summaried in Sec. III enable us to compute the elements of the initial-state density matrix [cf. (2.25)], which we now write in the form

$$\rho_{xx'}(\mathscr{I}\mathscr{S},\hat{\boldsymbol{\alpha}}) = \sum_{\Omega_{\mathscr{S}},\Omega_{\mathscr{I}}}\sum_i P_i(x;\mathscr{S}\Omega_{\mathscr{S}}\mathscr{I}\Omega_{\mathscr{I}}\,|\,i\rangle\langle i\,|\,x';\mathscr{S}\Omega_{\mathscr{S}}\mathscr{I}\Omega_{\mathscr{I}})\,, \tag{4.1}$$

with $|\,i\rangle = \underline{A}\,|\,nn'\rangle$ and $P_i = P_X(n)P_Y(n')$.

It is useful to recall several items discussed in Sec. II. For one thing, the electronic-nuclear spin matrix elements appearing in (4.1) are to be computed for some very large, fixed value of the internuclear separation. Secondly, angular kets such as $|\,i\rangle$ have the photon-frame quantization axis $\hat{\boldsymbol{\alpha}}$, whereas rounded kets such as $|\,x;\mathscr{S}\Omega_{\mathscr{S}}\mathscr{I}\Omega_{\mathscr{I}}\rangle$ have a laboratory-frame space quantization axis that is parallel to $\mathbf{k}$, the initial relative momentum of the colliding atoms. Furthermore, the computation of the density matrix can be performed treating the nuclei as if they were distinguishable. We may therefore associate nucleus A with atom X and nucleus B with atom Y and henceforth cease to distinguish between the labels A and X or B and Y. Finally. the set of molecular-type quantum numbers x includes Λ_x the projection quantum number of the component of electronic orbital angular momentum along $\hat{\mathbf{k}}$, but not the electronic and nuclear spin quantum numbers $\mathscr{S}$, $\Omega_{\mathscr{S}}$, $\mathscr{I}$ and $\Omega_{\mathscr{I}}$.

For simplicity, we consider a system such as Na $\cdots$ Na, in the pseudo-two-electron approximation. However, many of the results obtained here easily are generalized to situations involving more electrons than two, cf. the end of Sec. V.

The initial state $|\,i\rangle$ is the antisymmetrized product of two atomic hyperfine states,

$$|i\rangle = \underline{A}\,|n((LS)J)I,FM_F;A\rangle\,|n'((L'S')J')I',F'M_F';B\rangle$$
$$\equiv \underline{A}\,|\zeta FM_F;A\rangle\,|\zeta'F'M_F';B\rangle\ . \tag{4.2}$$

The quantum numbers appearing in these kets include those (L and S) for electronic orbital and spin angular momentum, J the total electronic angular momentum, and I the spin of the atomic nucleus. F and M_F are the quantum numbers associated with the magnitude and projection (along $\hat{\alpha}$) of the total atomic angular momentum. Finally, n is a label that distinguishes between different states which share common values of L, S, J, I, F, and M_F.

It is convenient at this point to introduce the laboratory-frame atomic orbital product states

$$\begin{aligned}|t;\mathscr{S}\Omega_{\mathscr{S}}\mathscr{I}\Omega_{\mathscr{I}}\rangle &= \underline{A}[\,|nL\Omega;A)\,|n'L'\Omega';B)\,|(SS')\mathscr{S}\Omega_{\mathscr{S}})] \\ &\quad\times|(II')\mathscr{I}\Omega_{\mathscr{I}})\ , \\ |\tilde{t};\mathscr{S}\Omega_{\mathscr{S}}\mathscr{I}\Omega_{\mathscr{I}}\rangle &= \underline{A}[\,|nL\tilde{\Omega};A)\,|n'L'\tilde{\Omega}';B)\,|(SS')\mathscr{S}\Omega_{\mathscr{S}})] \\ &\quad\times|(II')\mathscr{I}\Omega_{\mathscr{I}})\ ,\end{aligned} \tag{4.3}$$

so that the density matrix (4.1) can be rewritten as a sum of products

$$\rho_{xx'}(\mathscr{I}\mathscr{S},\hat{\alpha}) = \sum_{t,\tilde{t}} (\mathscr{S}x\,|\,\mathscr{S}t)(\mathscr{S}x'\,|\,\mathscr{S}\tilde{t})^* V(\mathscr{I}\mathscr{S}t\tilde{t}) \tag{4.4}$$

of laboratory-frame objects,

$$(\mathscr{S}x\,|\,\mathscr{S}t) = (x;\mathscr{S}\Omega_{\mathscr{S}}\mathscr{I}\Omega_{\mathscr{I}}\,|\,t;\mathscr{S}\Omega_{\mathscr{S}}\mathscr{I}\Omega_{\mathscr{I}})\ , \tag{4.5}$$

which are independent of the quantum numbers $\Omega_{\mathscr{S}}$, $\mathscr{I}$ and $\Omega_{\mathscr{I}}$, and the polarization-dependent objects

$$V(\mathscr{I}\mathscr{S}t\tilde{t}) = \sum_{\Omega_{\mathscr{S}},\Omega_{\mathscr{I}}}\sum_i P_i(t;\mathscr{S}\Omega_{\mathscr{S}}\mathscr{I}\Omega_{\mathscr{I}}\,|\,i\rangle \times\langle i\,|\,\tilde{t};\mathscr{S}\Omega_{\mathscr{S}}\mathscr{I}\Omega_{\mathscr{I}})\ . \tag{4.6}$$

For two-electron systems it is not at all difficult to obtain analytical expressions for the integrals $(\mathscr{S}x\,|\,\mathscr{S}t)$, cf. Appendix B. Thus, the main computational task is the evaluation of $V(\mathscr{I}\mathscr{S}t\tilde{t})$. (It is easily verified that the evaluation of V given here holds as long as each reactant is an effective one- or two-electron atom.) This is made somewhat easier by recognizing that the antisymmetrization operators appearing in the definitions of the bras and kets of (4.6) can be discarded without affecting the value of V.

The Euler angles of $\hat{\alpha}$ are $(\alpha,\beta,0)$ and those of the laboratory-frame space quantization axis $\hat{\mathbf{k}}$ are (0,0,0). In accordance with the rotation conventions of Messiah[16] it then follows that

$$|SS'\mathscr{S}\Omega_{\mathscr{S}}) = \underline{R}^{-1}(\alpha,\beta,0)\,|SS'\mathscr{S}\Omega_{\mathscr{S}}\rangle = \sum_{\Omega'_{\mathscr{S}}} \mathscr{R}^{\mathscr{S}}_{\Omega_{\mathscr{S}}\Omega'^{*}_{\mathscr{S}}}(\alpha,\beta,0)\,|SS'\mathscr{S}\Omega'_{\mathscr{S}}\rangle \tag{4.7}$$

and

$$|II'\mathscr{I}\Omega_{\mathscr{I}}) = \sum_{\Omega'_{\mathscr{I}}} \mathscr{R}^{\mathscr{I}}_{\Omega_{\mathscr{I}}\Omega'^{*}_{\mathscr{I}}}(\alpha,\beta,0)\,|II'\mathscr{I}\Omega'_{\mathscr{I}}\rangle\ . \tag{4.8}$$

By substituting these expressions into (4.6) and making use of the unitary property of the representation coefficients we find that

$$V(\mathscr{I}\mathscr{S}t\tilde{t}) = \sum_i P_i \sum_{M_{\mathscr{S}},M_{\mathscr{I}}} [\langle\mathscr{I}M_{\mathscr{I}}\,|\,\langle\mathscr{S}M_{\mathscr{S}}\,|\,(t\,|\,i\rangle] \times[\langle i\,|\,\tilde{t})\,|\,\mathscr{S}M_{\mathscr{S}}\rangle\,|\,\mathscr{I}M_{\mathscr{I}}\rangle]\ , \tag{4.9}$$

with $|\,t)$ and $|\,\tilde{t})$ denoting the unsymmetrized products of atomic orbitals

$$\begin{aligned}|\,t) &= |\,nL\Omega;A)\,|\,n'L'\Omega';B) \\ \text{and} \\ |\,\tilde{t}) &= |\,nL\tilde{\Omega};A)\,|\,n'L'\tilde{\Omega}';B)\end{aligned} \tag{4.10}$$

and where $|\,i\rangle$ is now unsymmetrized, in accordance with the remarks above.

The next step is to transform these two laboratory-frame kets into the photon frame, using the relationship

$$|nL\Omega;z) = \sum_M \mathscr{R}^{L\,*}_{\Omega M}(\alpha,\beta,0)\,|nLM;z\rangle,\quad z=A,B\ .$$

When this is done and the results substituted into (4.9) it is found that V may be written in the form

$$V(\mathscr{I}\mathscr{S}t\tilde{t}) = \sum_{T,\Omega_T,M_T} \mathscr{R}^{T}_{\Omega_T M_T}(\alpha,\beta,0)\left[\sum_{\mathscr{L},\mathscr{L}'} a(T\Omega_T,LL',\mathscr{L}\mathscr{L}',\{\Omega\}) \sum_{M_F,M'_F} [P(M_FM'_F)g(TM_T,\Gamma,\mathscr{L}\mathscr{L}',M_FM'_F)]\right], \tag{4.11}$$

where $P(M_F,M'_F)\equiv P(FM_F,F'M'_F)$ has been inserted in place of the less explicit $P_i = P_X(n)P_Y(n')$. The set $\{\Omega\}$ consists of the four quantum numbers, Ω, Ω', $\tilde{\Omega}$, and $\tilde{\Omega}'$ associated with t and $\tilde{t}$, $\Gamma=\{FF',JJ',II',SS',\mathscr{S}\mathscr{I}\}$, and

$$a(T\Omega_T,LL',\mathscr{L}\mathscr{L}',\{\Omega\}) = (-1)^{L+L'-\tilde{\Omega}-\tilde{\Omega}'}\langle\Omega\Omega'-\tilde{\Omega}-\tilde{\Omega}'\,|\,((LL')\mathscr{L},(LL')\mathscr{L}')T\Omega_T\rangle\ . \tag{4.12}$$

Finally, g is defined by

$$g(TM_T,\Gamma,\mathscr{L}\mathscr{L}',M_F M_F') = \sum_{\{M\}}\sum_{l,l'} \begin{bmatrix} L \\ l\tilde{M} \end{bmatrix} \begin{bmatrix} L' \\ l'\tilde{M}' \end{bmatrix} \langle MM'll' \,|\, ((LL')\mathscr{L},(LL')\mathscr{L}')TM_T \rangle \times \sum_{M_{\mathscr{S}},M_{\mathscr{I}}} (\langle \mathscr{I}M_{\mathscr{I}} \,|\, \langle \mathscr{S}M_{\mathscr{S}} \,|\, \langle b \,|\, i \rangle)(\langle i \,|\, \tilde{b} \rangle \,|\, \mathscr{S}\mathscr{M}_{\mathscr{S}} \rangle \,|\, \mathscr{I}M_{\mathscr{I}} \rangle) \tag{4.13}$$

with $\{M\}=(M,M',\tilde{M},\tilde{M}')$ and

$$|b\rangle = |nLM;A\rangle\,|n'L'M';B\rangle\ , \qquad |\tilde{b}\rangle = |nL\tilde{M};A\rangle\,|n'L'\tilde{M}';B\rangle\ . \tag{4.14}$$

The diagrammatic analysis is now applied to this function g. Using the rules presented in Sec. III we obtain for g the standard diagram

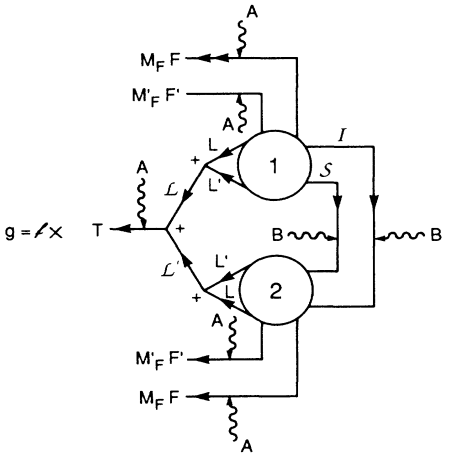

(4.15a)

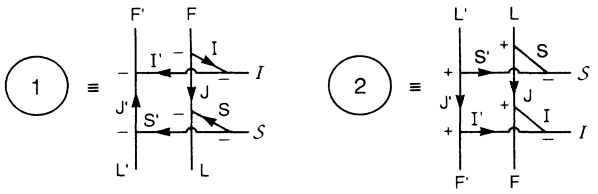

(4.15b)

wherein

$$\ell=(-1)^{L+L'+\mathscr{L}+2\mathscr{L}'}([\mathscr{L}][\mathscr{L}'][T])^{1/2} \times [F][F'][J][J'][\mathscr{I}][\mathscr{S}]\ . \tag{4.16}$$

Next we apply the expansion theorem at the five points marked A in (4.15a), using the GCGC $\langle (FF')\mathscr{F},(FF')\mathscr{F}',TM_T \,|\, M_F M_F,\tilde{M}_F,\tilde{M}_F \rangle$. Then (3.7) is applied at B in (4.15a) to yield the result

$$g=\ell \sum_{\mathscr{F},\mathscr{F}',Q} [Q][\mathscr{F}][\mathscr{F}']\underline{Q}(\Gamma;\mathscr{F}',\mathscr{F}) \times \underline{X}(\mathscr{F}\mathscr{F}',\mathscr{L}\mathscr{L}',Q,\Gamma)\ , \tag{4.17}$$

with $\underline{Q}$ and $\underline{X}$ defined by the following:

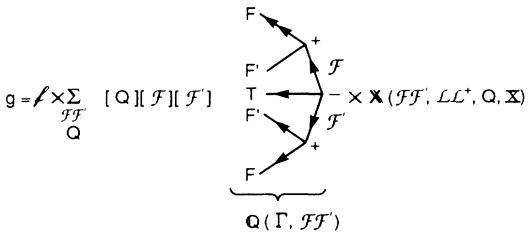

(4.18a)

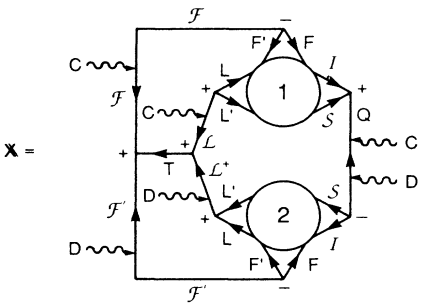

(4.18b)

The function $\underline{X}=\underline{X}(\mathscr{F}\mathscr{F}',\mathscr{L}\mathscr{L}',Q,\Gamma)$ can be separated into three simpler parts by applying the separation theorem at the points C of (4.18b) and again at the points D. This leads to the formula

$$\underline{X}(\mathscr{F}\mathscr{F}',\mathscr{L}\mathscr{L}',Q,\Gamma) = \underline{D}(\Gamma,\mathscr{L}\mathscr{F}Q)\underline{E}(\mathscr{F}\mathscr{F}',\mathscr{L}\mathscr{L}',QT)\underline{F}(\Gamma,\mathscr{L}'\mathscr{F}'Q)\ , \tag{4.19}$$

with $\underline{D}$, $\underline{E}$, and $\underline{F}$ defined by

$$\underline{D}=\left\{\begin{matrix} L & F & \mathscr{L} & \mathscr{F} & L' & F' \\ J & & Q & & J' & \\ S & I & \mathscr{S} & \mathscr{I} & S' & I' \end{matrix}\right\} \times(-1)^{2(J+\mathscr{F}+I+\mathscr{L})+(\mathscr{F}+Q+\mathscr{L})} \times(-1)^{(F+F'+\mathscr{F})+(I'+J'+F')+(I+J+F)}\ , \tag{4.20}$$

$$\underline{E}=\left\{\begin{matrix} \mathscr{F} & \mathscr{F}' & T \\ \mathscr{L}' & \mathscr{L} & Q \end{matrix}\right\}(-1)^{2\mathscr{F}+(\mathscr{F}+Q+\mathscr{L})+(\mathscr{F}'+Q+\mathscr{L}')} \tag{4.21}$$

and

$$\underline{F}=\begin{Bmatrix} F & L & \mathscr{F}' & \mathscr{L}' & F' & L' \\ & J & & Q & & J' \\ I & S & \mathscr{I} & \mathscr{S} & I' & S' \end{Bmatrix}$$

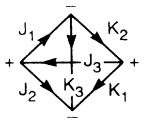

$$\equiv \begin{Bmatrix} J_1 & J_2 & J_3 \\ K_1 & K_2 & K_3 \end{Bmatrix} \equiv 6j \tag{4.23}$$

$$\times(-1)^{2(\mathscr{L}'+\mathscr{S}+\mathscr{F}')+(J+I+F)+(J'+I'+F')}$$

$$\times(-1)^{(Q+\mathscr{I}+\mathscr{S})+(Q+\mathscr{L}'+\mathscr{F}')+(L+L'+\mathscr{L}')} . \tag{4.22}$$

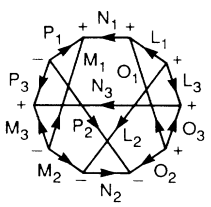

$$\equiv \begin{Bmatrix} L_1 & M_1 & L_2 & M_2 & L_3 & M_3 \\ & N_1 & & N_2 & & N_3 \\ O_1 & P_1 & O_2 & P_2 & O_3 & P_3 \end{Bmatrix} \equiv 15j .$$

The first objects occurring on the right-hand sides of these last three formulas are defined by the following equations:

The following identity can be verified:

$$\underline{Q}=([\mathscr{F}][\mathscr{F}'][T])^{-1/2}(-1)^{F+M_F+F'+M_F'}$$

$$\times(-1)^{(F+F'+\mathscr{F})+(\mathscr{F}+\mathscr{F}'+T)+2(F+\mathscr{F}')}\langle M_F M_F'-M_F-M_F' \mid ((FF')\mathscr{F},(FF')\mathscr{F}')TM_T\rangle . \tag{4.24}$$

By combining these results we obtain for g the formula

$$g(TM_T,\Gamma,\mathscr{L}\mathscr{L}',M_F M_F')$$

$$=(-1)^{F+M_F+F'+M_F'}\sum_{\mathscr{F},\mathscr{F}'}\phi\langle M_F M_F'-M_F-M_F' \mid ((FF')\mathscr{F},(FF')\mathscr{F}')TM_T\rangle$$

$$\times\sum_{Q}\begin{Bmatrix} L & F & \mathscr{L} & \mathscr{F} & L' & F' \\ & J & & Q & & J' \\ S & I & \mathscr{S} & \mathscr{I} & S' & I' \end{Bmatrix}\begin{Bmatrix} F & L & \mathscr{F}' & \mathscr{L}' & F' & L' \\ & J & & Q & & J' \\ I & S & \mathscr{I} & \mathscr{S} & I' & S' \end{Bmatrix}$$

$$\times\begin{Bmatrix} \mathscr{F} & \mathscr{F}' & T \\ \mathscr{L}' & \mathscr{L} & Q \end{Bmatrix}[Q] , \tag{4.25}$$

with

$$\phi=([\mathscr{L}][\mathscr{L}'][\mathscr{F}][\mathscr{F}'])^{1/2}[F][F'][J][J'][\mathscr{I}][\mathscr{S}](-1)^{(\mathscr{F}+\mathscr{F}'+T)+(Q+\mathscr{I}+\mathscr{S})+2(J+I'+F+\mathscr{S}+\mathscr{I})+2(L+L'+\mathscr{L})} . \tag{4.26}$$

All of the objects occurring in (4.26) can be computed readily. Therefore, the task of reducing the evaluation of the density matrix to manageable proportions has come to an end. The GCGC appearing in (4.25) is different from zero only if $M_T=0$. This reduces to a single term the sum on this quantum number appearing in the formula (4.11) for $V(\mathscr{I}\mathscr{S}t\tilde{t})$.

V. SYMMETRY CONSIDERATIONS

By exploiting the properties of the various factors [e.g., $(\mathscr{S}x \mid \mathscr{S}t)$, P_i, a and g] that contribute to the density matrix (4.4), one can obtain a number of useful conclusions about polarization-dependent collisions. These conclusions, which are examined in this section, pertain both to the functional dependence of the integral cross section upon $\hat{\alpha}$ [$\equiv(\alpha,\beta,0)$] and to the populations of the various electronic initial states.

We begin by establishing some limits on T, the degree of the associated Legendre polynomial to which the representation coefficient

$$\mathscr{R}^T_{\Omega_T 0}(\alpha,\beta,0)=(-1)^{\Omega_T}[4\pi/(2T+1)]^{1/2}Y_{T,-\Omega_T}(\beta,\alpha) \tag{5.1}$$

is proportional. Because the GCGC occurring in the definition (4.12) of a contains a factor proportional to the Kronecker delta $\delta_{\mathrm{Kr}}(\Omega_T \mid (\Omega+\Omega')-(\tilde{\Omega}+\tilde{\Omega}'))$, it follows that

$$T\geq\Omega_T=(\Omega+\Omega')-(\tilde{\Omega}+\tilde{\Omega}') . \tag{5.2}$$

Consider next the $6j$ symbol $\{\begin{smallmatrix} \mathscr{I} & \mathscr{F}' & T \\ \mathscr{L}' & \mathscr{S} & Q \end{smallmatrix}\}$ which occurs in the formula (4.25) for g. Because the angular momentum quantum numbers at each node [cf. (4.23)] must satisfy the "triangle rule," T is further restricted by the conditions

$$T \leq \min(\mathcal{F}+\mathcal{F}', \mathcal{L}+\mathcal{L}') \leq \min(2(F+F'), 2(L+L')) \ . \tag{5.3}$$

The conditions (5.2) and (5.3) severely restrict the allowable values of T. A simple example is a collision between two Na($(3p)^2P$) atoms. In this case $L=L'=1$ and so T can be no greater than 4. However, if the experiment is so arranged that these two atoms are prepared in hyperfine states with $F=F'=0$, then the only allowed value of T is zero and the cross section will be independent of the laser polarization. This illustrates a general rule—that the polarization dependences of the integral cross section are intimately related to the atomic hyperfine structure, whereas the dynamics of the state-to-state transitions depend only upon the atomic quantum numbers L, L', $\mathcal{S}$ and (for indistinguishable nuclei) $\mathcal{I}$. This fact may be useful in designing experiments to uncover the mechanisms of complex atomic reactions (cf. Sec. VI).

The quantity $\Omega+\Omega'$ that appears in (5.2) is the sum of the electronic orbital angular momentum projection quantum numbers of the two atomic orbitals associated with the product state $|t)$ of (4.10); $(\tilde{\Omega}+\tilde{\Omega}')$ is the analogous quantity associated with the product state $|\tilde{t})$. Returning now to (4.4) and (4.5) we see that the only states $|t)$ and $|\tilde{t})$ which contribute to the density matrix are those for which $\Omega+\Omega'=\Lambda_x$ and $\tilde{\Omega}+\tilde{\Omega}'=\Lambda_{x'}$. Therefore, when the axial projection quantum numbers of the two quasimolecular states x and x' are equal, the only value of Ω_T which contributes to $\rho_{xx'}(\mathcal{I}\mathcal{S},\hat{\alpha})$ is $\Omega_T=0$. The polarization dependence of the density matrix is then a dependence upon the second Euler angle $\beta=\theta$, which occurs in the Legendre polynomials $\mathscr{R}^T_{00}(\alpha\beta 0)=P_T(\cos\beta)$. This is an important observation because we already have seen in Sec. II that $\sigma^{(\pm)}_{xx'}(\mathcal{S},E) \propto \delta_{\Lambda_x\Lambda_{x'}}$. Consequently, the only contributions to the integral cross section for AI [cf. (2.24)] will be from pairs of quasimolecular states with $\Lambda_x=\Lambda_{x'}$ and the cross section itself will be represented by the Legendre polynomial series

$$\rho_{xx'}(\mathcal{I}\mathcal{S},\hat{\alpha}) = \sum_T P_T(\cos\beta)\rho^T_{xx'}(\mathcal{I}\mathcal{S}) \ , \tag{5.4}$$

with

$$\rho^T_{xx'}(\mathcal{I}\mathcal{S}) = \sum_{t,\tilde{t}} (\mathcal{S}x \mid \mathcal{S}t)(\mathcal{S}\tilde{t} \mid \mathcal{S}x') \sum_{\mathcal{L},\mathcal{L}'} a(T0,LL',\mathcal{L}\mathcal{L}',\{\Omega\}) \sum_{M_F,M_F'} P(M_F,M_F')g(T0,\mathcal{L}\mathcal{L}',M_FM_F') \ . \tag{5.5}$$

We next consider the special case of initial states for which

$$P(FM_F,F'M_F') = P(F-M_F,F'-M_F') \ . \tag{5.6}$$

Among the many experimental situations to which this condition applies is the excitation of ground-state Na atoms by linearly polarized D_2-line radiation resonant with the $(F=2\rightarrow F=3)$ hyperfine transition. By using the identity

$$\begin{aligned}\langle M_FM_F'-M_F-M_F' \mid ((FF')\mathcal{F},(FF')\mathcal{F}'),T0\rangle \\ =(-1)^{2(F+F')+T} \\ \times\langle -M_F-M_F'M_FM_F' \mid ((FF')\mathcal{F},(FF')\mathcal{F}'),T0\rangle\end{aligned} \tag{5.7}$$

in conjunction with the formula (4.25) we find that

$$\begin{aligned}g(T0,\Gamma,\mathcal{L}\mathcal{L}',M_FM_F') \\ =(-1)^{2(F+F')+T}g(T0,\Gamma,\mathcal{L}\mathcal{L}',-M_F-M_F') \ .\end{aligned} \tag{5.8}$$

Consequently, the factor

$$G \equiv \sum_{M_F,M_F'} P(M_F,M_F')g(T0,\Gamma,\mathcal{L}\mathcal{L}',M_FM_F') \ , \tag{5.9}$$

which occurs in $V(\mathcal{I}\mathcal{S}t\tilde{t})$, cf. (4.11), can be written in the form $G=G\nu(2(F+F')+T)$ where $\nu(n)=\frac{1}{2}[1+(-1)^n]$ is 0 or 1 depending on whether the integer n is odd or even.

The conclusion which can be drawn from this is that when the condition (5.6) is satisfied, the only nonzero contributions to $V(\mathcal{I}\mathcal{S}t\tilde{t})$ are from values of T for which $T+2(F+F')$ is an even integer. In the Na preparation mentioned above $F=F'=3$, so that the only contributors are even integral values of T. However, if one but not both of F and F' were half integral, the only nonzero contributors to V would be odd-integral values of T.

Let us next focus our attention upon two "atomic states," $|t)$ and $|\tilde{t})$, [or two "molecular states," $|p)$ and $|p')$] with the respective angular momentum projection quantum numbers (Ω,Ω') and $(\tilde{\Omega},\tilde{\Omega}')$ [or Λ_p and $\Lambda_{p'}$] which are equal but of opposite algebraic sign, that is, $\tilde{\Omega}=-\Omega$ and $\tilde{\Omega}'=-\Omega'$. Then, analogous to (5.7) is the relationship

$$\begin{aligned}\langle \Omega\Omega',-\tilde{\Omega}-\tilde{\Omega}' \mid ((LL')\mathcal{L},(LL')\mathcal{L}')T,\Omega+\Omega'-\tilde{\Omega}-\tilde{\Omega}'\rangle \\ =(-1)^T\langle -\Omega-\Omega',\tilde{\Omega}\,\tilde{\Omega}' \mid ((LL')\mathcal{L},(LL')\mathcal{L}') \\ \times T,-\Omega-\Omega'+\tilde{\Omega}+\tilde{\Omega}'\rangle \ .\end{aligned} \tag{5.10}$$

It follows from this that when the only contributors to (4.11) are even integral values of T (namely, when $F+F'$ is an integer),

$$\rho_{tt}=\rho_{t't'} \ (\rho_{pp}=\rho_{p'p'}) \ . \tag{5.11}$$

To obtain this result we have used the facts that $M_T=0$ in (4.11) and that the only elements of the density matrix that contribute to the integral cross section are those for which $\Omega_T=0$ in (4.11). An example of this is provided by the previously mentioned excitation of Na atoms by linearly polarized light; according to (5.9) the polarization dependence of the two molecular states $|p)=\underline{A}\{[\,|\sigma_g)\,|\pi_u^1)-|\sigma_u)\,|\pi_g^1)]\,|\mathcal{S}\Omega_{\mathcal{S}})\}$ and $|p')=\underline{A}\{[\,|\sigma_g)\,|\pi_u^{-1})-|\sigma_u)\,|\pi_g^{-1})]\,|\mathcal{S}\Omega_{\mathcal{S}})\}$ will be identical.

A rather obvious but nevertheless important observation is that the isotropic part of $P(FM_F,F'M_F')$, namely, the part which is independent of M_F and M_F', contributes nothing to the polarization dependence of the reaction cross section. Thus, the part of $V(\mathscr{I}\mathscr{S}t\tilde{t})$ associated with the isotropic (I) part of $P(FM_F,F'M_F')\equiv P_I+\delta P(FM_F,F'M_F')$ is given by the expression

$$V_I(\mathscr{I}\mathscr{S}t\tilde{t})=P_I\sum_{\mathscr{L}}a(00,LL',\mathscr{L}\mathscr{L},\{\Omega\})g'(\Gamma,\mathscr{L}\mathscr{L}) , \tag{5.12}$$

with

$$g'(\Gamma,\mathscr{L}\mathscr{L})=\sum_{\mathscr{F},Q}\phi\begin{Bmatrix} L & F & \mathscr{L} & \mathscr{F} & L' & F' \\ & J & & Q & & J' & \\ S & I & \mathscr{S} & \mathscr{I} & S' & I' \end{Bmatrix} \times\begin{Bmatrix} F & L & \mathscr{F} & \mathscr{L} & F' & L' \\ & J & & Q & & J' & \\ I & S & \mathscr{I} & \mathscr{S} & I' & S' \end{Bmatrix} \times[\mathscr{F}]^{1/2}[Q] \tag{5.13}$$

and where ϕ, cf. (4.26), is to be evaluated with $\mathscr{L}'=\mathscr{L}$. This result is a direct consequence of the formulas of Sec. IV and the identity

$$\sum_{M_F,M_F'}\langle M_FM_F'-M_F-M_F' \mid ((FF')\mathscr{F},(FF')\mathscr{F}')T0\rangle \times(-1)^{F+M_F+F'+M_F'}=[\mathscr{F}]^{1/2}\delta_{\mathscr{F}\mathscr{F}'}\delta_{T0} , \tag{5.14}$$

which is satisfied provided that F, F', and $\mathscr{F}$ from a triangle. Clearly, a necessary condition for polarization dependence is that at least two of the factors $P(FM_F,F'M_F')$ be different from one another.

The last rule to be considered pertains to the special case defined by the conditions

$$\begin{aligned} &F=L+S+I , \\ &F'=L'+S'+I' , \\ &P(FM_F,F'M_F')=\delta_{M_F,\pm F}\delta_{M_F'\pm F'} . \end{aligned} \tag{5.15}$$

This unusual population can be produced experimentally (at least for the geometry $\beta=\pi/2$) by excitation with a circularly polarized laser. It is a remarkable fact that $\mathscr{S}$, the total electron spin quantum number associated with the population (5.15) of atomic states, is restricted to the single value of $S+S'$. This is of great practical value because it identifies the condition for preparing pairs of atoms in a single, pure spin state, namely, that with $\mathscr{S}=S+S'$. It provides a filter for experimentally separating the reactive contributions of these "maximum-spin states" from those of all others; in Na-Na collisions it separates the triplet states from the single states.

A proof of this rule can be obtained by examining the formula (4.25). From the conditions (5.15) it follows that $\mathscr{F}=\mathscr{F}'=F+F'$. The triangle conditions on the triples $\{\mathscr{F},Q,\mathscr{L}'\}$, $\{\mathscr{F}',Q,\mathscr{L}\}$, and $\{\mathscr{S},\mathscr{I},Q\}$ then require that

$$F+F'-L-L'\le Q\le F+F'+L+L' \tag{5.16a}$$

and

$$|\mathscr{I}-\mathscr{S}|\le Q\le\mathscr{I}+\mathscr{S} \tag{5.16b}$$

These two ranges overlap only if $\mathscr{I}=\mathscr{I}_{\max}=I+I'$ and $\mathscr{S}=\mathscr{S}_{\max}=S+S'$, in which case the overlap is restricted to the single value $Q=\mathscr{I}_{\max}+\mathscr{S}_{\max}=(I+I')+(S+S')$. Thus, $V(\mathscr{I}\mathscr{S}t\tilde{t})$, and the density matrix itself, are zero unless $\mathscr{I}=I+I'$ and $\mathscr{S}=S+S'$.

This result has a very simple interpretation in terms of the vector-model picture for the addition of angular momenta. The condition (5.15) amounts to the assertion that all of the angular momentum vectors **L**, **L'**, **S**, **S'**, **I**, **I'**, **J**, **J'**, **F**, and **F'** are colinear. In this special case the recoupling of the vectors is a trivial task leading directly to $\mathscr{I}=I+I'$ and $\mathscr{S}=S+S'$.

It is well to conclude our formal analysis with some general remarks on the results obtained and their applicability. While the discussion here has been cast in terms of AI, the results obtained can be applied to other processes without much difficulty. Indeed, the analysis of Secs. IV and V can be carried through for any atomic scattering process in which the electronic and nuclear spins are conserved and each atom effectively has less than three electrons. However, it is important to remember that (5.4) is valid only if $\Lambda_x=\Lambda_{x'}$. This equality follows immediately from the conservation of angular momentum for any *field-free* process; it may not hold exactly for laser-induced processes.

The other equations required for the construction of a general theory are (2.13) and (2.15), which are generally valid, and

$$\sigma_{pp'}(E,f)=\left[\frac{m_f}{2\pi\hbar^2}\right]^2\sum_f\int d\mathbf{k}\langle f \mid T \mid \mathbf{k}p\rangle P(\mathbf{k}) \times(v_f/v)\langle \mathbf{k}p' \mid T \mid f\rangle . \tag{2.14'}$$

Here, in contrast to (2.14), we do not specify the final-state quantum numbers f, except to note that they must include $\mathscr{S}$, $\Omega_{\mathscr{S}}$, $\mathscr{I}$, and $\Omega_{\mathscr{I}}$. Indeed, f may include a particular final velocity vector $\mathbf{v}_\gamma$. Given (2.13), (2.14'), and the results of Secs. IV and V, one can investigate the polarization dependence of any (spin-conserving) atomic process. It should be pointed out, however, that the details of arguments regarding selection rules and the effects of nuclear statistics are process dependent; these must be investigated separately. Finally, it must be remembered that our results are specific to the case of a single exciting laser or to two with a common photon frame.

VI. APPLICATION TO THE EXPERIMENTS INVOLVING POLARIZATION-DEPENDENT AI

As we have pointed out in Sec. I, it is observed experimentally that the integral cross section for the associative

ionization process $2\mathrm{Na}((3p)^2P_{3/2}) \rightarrow \mathrm{Na}_2^+(X\,^2\Sigma_g^+) + e^-$ depends on the polarization of the laser used to prepare the initial state. The theory which has been developed here enables us to turn measured values of this polarization dependence into tools for determining the state-specific cross sections $\sigma_{xx}^{(\pm)}(\mathscr{S})$, and, if they occur, the interference cross sections $\sigma_{xx'}^{(\pm)}(\mathscr{S})$, $x \neq x'$, as well. Our method is of value not only because it is complementary to purely numerical calculations but also because accurate computations of the state-specific cross sections are so very difficult to perform.

In this section the data of Fig. 1 will be used, together with theoretically derived information about Na_2 potential energy curves, to extract information about the reactive states which contribute to the measured rate of associative ionization. We begin by making a number of imprecise, but definite, conclusions about the characters of the reactive states. We then proceed to more specific but less reliable conclusions. The section ends with suggestions of experiments which might aid in refining the analysis, thereby further elucidating the reaction mechanism.

A. Qualitative considerations

The quasimolecular initial states considered here are listed in Table I. This set consists of all which correlate asymptotically with the configuration, $\mathrm{Na}(3p)+\mathrm{Na}(3p)$, except for Δ states. These apparently are quite unenergetic[18] and so, for the reasons stated in the final paragraph of Sec. II, cannot contribute to the rate of AI measured at moderate temperatures. Our general conclusions will be based upon the selection rules of Sec. II and the polarization dependences of the "single-state" density matrix components $\rho_{xx}^e(\mathscr{S},\hat{\alpha}) = \sum_{\mathscr{I}_e} \rho_{xx}(\mathscr{I}\mathscr{S},\hat{\alpha})$ and $\rho_{xx}^o(\mathscr{S},\hat{\alpha}) = \sum_{\mathscr{I}_o} \rho_{xx}(\mathscr{I}\mathscr{S},\hat{\alpha})$, shown in Fig. 2. The procedure for calculating these quantities, given $V(\mathscr{I}\mathscr{S}t\bar{t})$, is summarized in Appendix B.

The curves of Fig. 2 show the polarization dependence that would be observed if only one state were reactive. Curves labeled "even" refer to values of $\rho_{xx}^e(\mathscr{S},\hat{\alpha})$, and those labeled "odd" refer to $\rho_{xx}^o(\mathscr{S},\hat{\alpha})$. Since $\sigma_{xx}^{(+)}$ and $\sigma_{xx}^{(-)}$ are both positive valued, it is clear that no single electronic state can account for the experimentally observed polarization dependence of the AI integral cross section. In particular, we will see that no one of these states can reproduce the flat portion of the experimental curves (cf. Fig. 1) which extends from $\beta = 60°$ to 90°.

This simple line of argumentation can be carried further; the selection rules of Sec. II indicate that of the states listed in Table I, only the two pairs (a,c) and (b,f) can have nonzero interference cross sections. Given these facts it follows that

(1) the π^2 state (c–f of Table I) alone are unable to account for the observed polarization dependence of $\sigma(\hat{\alpha},E)$. These states, without others, would give rise to an integral cross section that *in*creased with increasing β.

(2) The σ^2 states (a and b of Table I) cannot account for the experimental observations. Without contributions from others these states produce a cross section which decreases too rapidly with increasing β.

(3) The $\sigma\pi$ states (g–j of Table I) are incapable, without others, of accounting for the flat portion of the $\sigma(\hat{\alpha},E)$ curve extending from $\beta = 60°$ to 90° [see comment after item (4)], and also fail to account for the rate of decrease of the experimental curves from $\beta = 0°$ to 40°.

(4) For the second reason in (3), no combination of π^2 and $\sigma\pi$ states can reproduce the observed polarization dependences.

(5) No combination of σ^2 and $\sigma\pi$ can reproduce the observed polarization dependence in the region $\beta = 60°$ to 90°. This is the weakest of our qualtiative conclusions, for it depends most strongly on the accuracy of the theoretical and experimental curves. However, it can be seen from Fig. 2 that *each* of the σ^2 and $\sigma\pi$ theoretical plots does indeed fall more quickly near $\beta = 90°$ than $\rho_{xx}(0)\sigma_{\mathrm{expt}}(\beta)$ (represented by a dashed line, within an overall additive constant). This observation, along with the normalization conditions $\sigma_{\mathrm{expt}}(0) = \sum \rho_{xx}(0)\sigma_{xx}(E)$

TABLE I. Quasimolecular states of Na_2 which correlate asymptotically with $\mathrm{Na}(3p)+\mathrm{Na}(3p)$. The polarization dependence of column 4 refers to the variation with the angle β (between the beam axis and the polarization of the laser) of a corresponding diagonal element of the density matrix.

Label	Asymptotic configuration	Term symbol	Polarization dependence (see caption)	Comments
a	σ_g^2-σ_u^2	$^1\Sigma_g^+$	Falling	Same term as c
b	$\sigma_g\sigma_u$-$\sigma_u\sigma_g$	$^3\Sigma_u^+$	Falling	Same term as f; large nuclear statistics effect
c	$\pi_g^1\pi_g^{-1}$-$\pi_u^1\pi_u^{-1}$	$^1\Sigma_g^+$	Rising	Same term as a
d	$\pi_g^1\pi_g^{-1}$-$\pi_u^1\pi_u^{-1}$	$^3\Sigma_g^-$	Rising	
e	$\pi_g^1\pi_u^{-1}$-$\pi_g^{-1}\pi_u^1$	$^1\Sigma_u^-$	Rising	
f	$\pi_g^1\pi_u^{-1}$-$\pi_g^{-1}\pi_u^{-1}$	$^3\Sigma_u^+$	Rising	Same term as b; large nuclear statistics effect
g	$\sigma_g\pi_u^{\pm1}$-$\sigma_u\pi_g^{\pm1}$	$^1\Pi_u$	Flat	
h	$\sigma_g\pi_u^{\pm1}$-$\sigma_u\pi_g^{\pm1}$	$^3\Pi_u$	Flat	Large nuclear statistics effect
i	$\sigma_g\pi_g^{\pm1}$-$\sigma_u\pi_u^{\pm1}$	$^1\Pi_g$	Flat	Very weakly populated
j	$\sigma_g\pi_g^{\pm1}$-$\sigma_u\pi_u^{\pm1}$	$^3\Pi_g$	Flat	

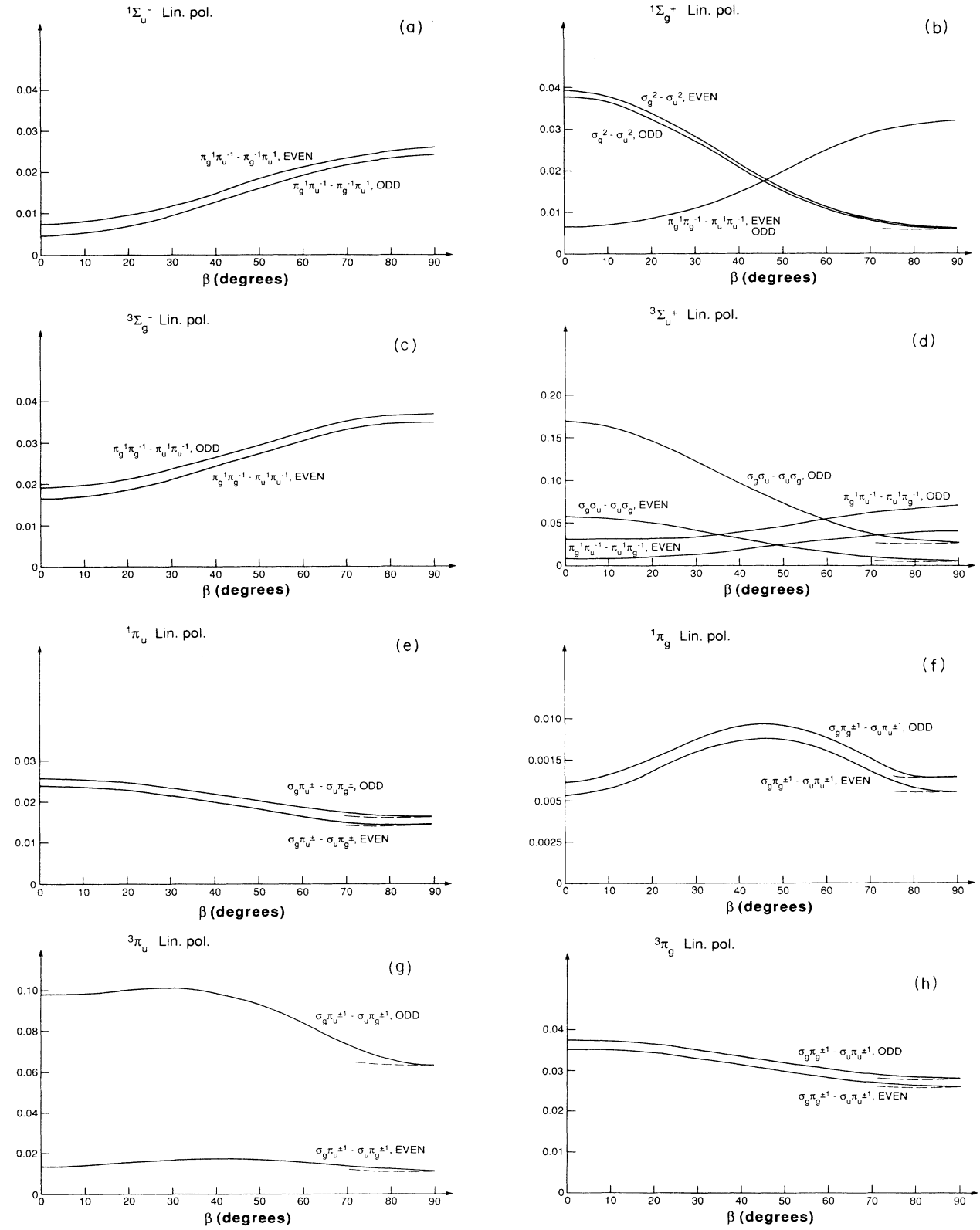

FIG. 2. Polarization dependence for the populated quasimolecular states [which correlate with Na($3p$) $\cdots$ Na($3p$)] that are listed in Table I. The numerical value of the ordinate is given by $\rho^o_{xx}(\mathscr{S},\beta)$ (curves labeled "odd"), or $\rho^e_{xx}(\mathscr{S},\beta)$ (curves labeled "even"). β is the angle between the photon frame (see text) and the direction of initial relative velocity. A dashed line indicates the experimental polarization dependence near $\beta=90°$ plotted on the same scale.

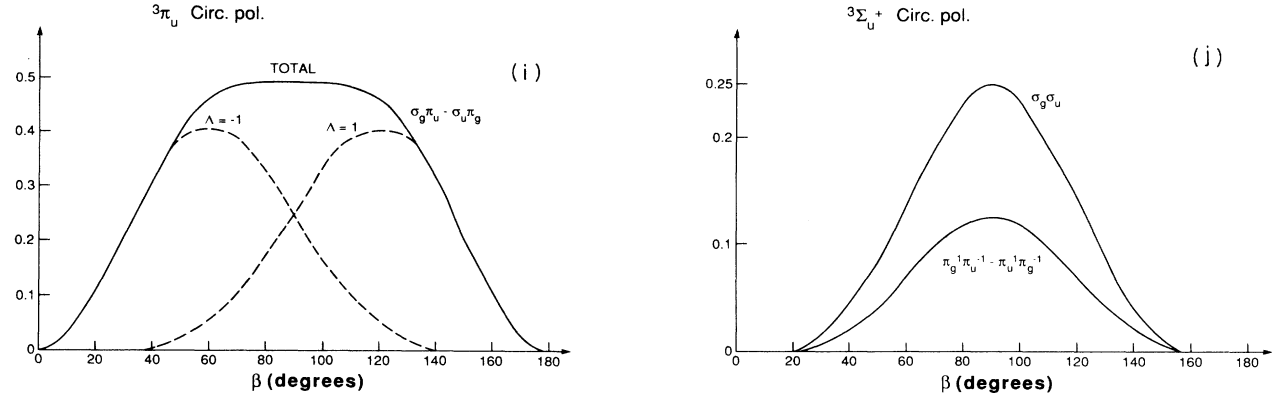

FIG. 2. (*Continued*).

$=1$ ($x=\sigma^2$, $\sigma\pi$ states), leads directly to the stated conclusion.

We can add to these conclusions one which follows from a separate experiment in which Na atoms were excited by *circularly* polarized D_2-line radiation, resonant with the ($F=2\rightarrow F=3$) hyperfine transition. The occurrence of associative ionization was observed.[19] To appreciate the significance of this one also must know that Hertel and his co-workers[11] have shown that the hyperfine distributions $P(FM_F)$ and $P'(F'M')$ appropriate to this situation are δ_{F,M_F} and $\delta_{F',M_F'}$, respectively, with $F=F'=3$. According to the last of the rules obtained in Sec. V, only triplet states can exist under these conditions. Thus, we conclude that

(6) At least one triplet state is a contributor to the associative ionization of two Na ($(3p)^2P_{3/2}$) atoms.

The final entry in this list is a consequence of the approximate selection rule (2.33), according to which the reflection quantum number of a Σ electronic initial state must be the same as that of a Σ-state product ion. The only conceivable ionic product is $Na_2^+(X\,^2\Sigma_g^+)$ and so

(7) Cross sections specific to Σ^- initial states should be negligibly small.

Our qualitative findings can be summarized as follows: at least two quasimolecular states of Na_2 participate in the AI process, $2Na(3p)\rightarrow Na_2^+ + e^-$; at least one of these has the asymptotic configuration σ^2; at least one the configuration π^2; at least one is a triplet; and Σ^- initial states (such as d and e) are not expected to be significant contributors.

B. Quantitative considerations

Our next objective is to obtain numerical estimates of the state-to-state cross sections which contribute to the measured rate of AI. The first step in this direction is to determine which electronic states are able to participate. The qualitative findings of Sec. VI A somewhat limit the field but to proceed further we must have some idea of which molecular channels are open. This requires quantitative information about the adiabatic potential energy curves of the ten Na_2 states listed in Table I. The validity of the conclusions which we can make will depend upon the accuracy of the potential curves used in our calculations. However, the demands of the analysis are not terribly exacting; we simply need to know whether and where these curves intersect that of $Na_2^+(X\,^2\Sigma_g^+)$ ion.

Our first attempt to analyze this problem was based upon the single potential energy curve[17] (the dotted line in Fig. 3) for which information then was available. This curve subsequently was found to be so inaccurate that our analysis was completely invalidated. The more recent and presumably more reliable potential energy curves which we use here are those of Henriet, Masnou-Seeuws, and LeSech[20] some of which are shown in Fig. 3. For the two $^1\Sigma_g^+$ states shown in Fig. 3, we have assumed that the higher in energy is dominated by π^2 (rather than σ^2) configurations at large internuclear separations. A similar assumption is made for the two $^3\Sigma_u^+$ states. We shall proceed without questioning the accuracy of these curves but the analysis will be presented in a way which easily could be adapted to another set of curves should a reason

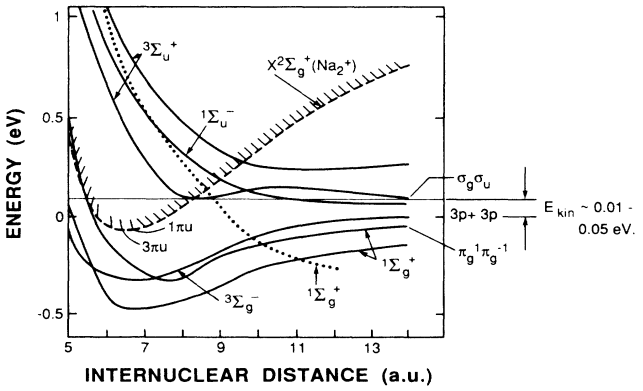

FIG. 3. Potential energy surfaces for some states of Na · · · Na which asymptotically correlate to the 2Na($3p$) limit, and the potential energy surface associated with the $(X\,^2\Sigma_g^+)Na_2^+$ ion, after Ref. 20. The asymptotic assignments $\sigma_g\sigma_u(^3\Sigma_u^+)$ and $\pi_g^1\pi_g^{-1}(^1\Sigma_g^+)$ have been assumed.

TABLE II. Legendre polynomial expansion coefficients of the density-matrix elements, defined by (6.4).

State label [cf. (6.1)] α	a_α	b_α	c_α
1	0.09074	0.1217	0.01905
2	0.0452	−0.03263	0.003174
3	0.03781	0.01236	0
4	0.03781	0.03263	−0.01905

for doing so ever be found (cf. discussion at end of this section).

Curves with classical turning points which do not lie in the $Na_2^+ + e^-$ continuum are assumed to be unreactive (cf. final paragraph of Sec. II). This energetic criterion, together with the approximate selection rule responsible for item (6) of Sec. VI A, limits the contending states to the following four:

$$\begin{aligned}&(1)\ {}^3\Sigma_u^+(\sigma_g\sigma_u),\ b \text{ from Table I}\\ &(2)\ {}^1\Sigma_g^+(\pi_g^1\pi_g^{-1}),\ c \text{ from Table I}\\ &(3)\ {}^1\Pi_u(\sigma_g\pi_u^{\pm1}),\ g \text{ from Table I}\\ &(4)\ {}^3\Pi_u(\sigma_g\pi_u^{\pm1}),\ h \text{ from Table I}\ .\end{aligned} \tag{6.1}$$

According to the selection rules of Sec. II, there are no interference cross sections associated with these four states.

Furthermore, we ignore the effects of nuclear statistics by setting

$$\sigma_{xx}^{(+)}(\mathscr{S},E)\doteq\sigma_{xx}^{(-)}(\mathscr{S},E)\equiv\sigma_\alpha(E),\quad \alpha=(x,\mathscr{S})\ . \tag{6.2}$$

This is tantamount to assuming that the state-to-state cross sections depend only weakly upon Q, the orbital angular momentum quantum number of the product diatomic ion, cf. the discussion of Sec. II.

Subject to these restrictions and approximations, the cross-section formula (2.24) becomes

$$\sigma(\hat{\boldsymbol{\alpha}},E)=\sum_\alpha \sigma_\alpha(E)\rho_\alpha(\hat{\boldsymbol{\alpha}}) \tag{6.3}$$

with

$$\rho_\alpha(\hat{\boldsymbol{\alpha}})\equiv\sum_{\mathscr{S}}\rho_{xx}(\mathscr{S}\mathscr{S},\hat{\boldsymbol{\alpha}})\equiv a_\alpha P_0+b_\alpha P_2+c_\alpha P_4 \tag{6.4}$$

and where P_n denotes the Legendre polynomial $P_n(\cos\beta)$. Therefore,

$$\begin{aligned}\sigma(\hat{\boldsymbol{\alpha}},E)&=\Big[\sum_\alpha a_\alpha\sigma_\alpha\Big]P_0+\Big[\sum_\alpha b_\alpha\sigma_\alpha\Big]P_2\\ &\quad+\Big[\sum_\alpha c_\alpha\sigma_\alpha\Big]P_4\\ &\equiv\sum_{n=0,2,4} q_n(E)P_n(\cos\beta)\ .\end{aligned} \tag{6.5}$$

The procedure for computing the coefficients a_α, b_α, and c_α, defined by (6.4) is summarized in Appendix B. Their numerical values are listed in Table II. The coefficients $q_n(E)$, defined by (6.5), are obtained from measurements of the integral cross section $\sigma(\hat{\boldsymbol{\alpha}},E)$. Values specific to two different beam energies are listed in Table III.

The procedure for determining the cross section σ_α is straightforward: (6.5) provides three equations which the set of four σ_α's must satisfy, subject to the constraints

$$\sigma_\alpha(E)\geq 0,\quad \alpha=1,2,3,4\ . \tag{6.6}$$

These equations and constraints are so restrictive that we are able to draw quite definite conclusions about the relative magnitude of the state-specific cross sections. The results of the calculations are given in Table IV. The blank entries are indicative of the fact that the data for $v=5.2\times10^4$ cm sec^{-1} do not yield reliable estimates of the two very small cross sections σ_3 and σ_4. The zero entries for $v=1.56\times10^5$ cm sec^{-1} indicate that σ_3 and σ_4 are at least an order of magnitude smaller than σ_1.

C. Summary and concluding remarks

We conclude by briefly reviewing our current knowledge of the mechanism of the AI reaction $2Na(3\,^2P_{3/2})\rightarrow Na_2^+(X\,^2\Sigma_g^+)+e^-$ and by considering the outlook for further progress in this direction. One can conclude with certainty that at least two ABO electronic states participate in the reaction, that at least one of these is a triplet, and that both σ^2 and π^2 configurations must be reactive. Finally, as part of our symmetry analysis, we have found that Σ^- terms are very unlikely reactants. One ${}^3\Sigma_u^+$ state and one ${}^1\Sigma_g^+$ state tentatively have been identified as the dominant contributors. However, this last conclusion is dependent on rather uncertain information about the Na $\cdots$ Na energy levels.

The implication of the preceding sentence is that current information about the Na_2 energy levels still may be insufficient to insure the accuracy of our quantitative conclusions. Indeed, the most recent communication from Henriet and Masnou-Seeuws[18] indicates that of the states which correlate asymptotically with $2Na(3p)$ only two have potential energy curves which intersect that of the $X\,^2\Sigma_g^+$ of Na_2^+ and that one of these is a ${}^1\Sigma_u^-$ state.

TABLE III. Legendre polynomial expansion coefficients of the integral cross section, defined according to (6.5). v is the average velocity of the beam atoms.

v (cm sec^{-1})	q_0	q_2	q_4
5.2×10^4	0.7341	0.2192±0.003	0.0466±0.005
1.56×10^5	0.6516	0.2585±0.004	0.0885±0.003

TABLE IV. State-specific cross sections for AI. The states are labeled according to (6.1).

v (cm sec^{-1})	σ_2/σ_1	σ_3	σ_4
5.2×10^4	1.8		
1.56×10^5	1.7	0	0

According to our theory reaction from this state is disallowed by symmetry considerations. This would leave only one strongly reactive state, a situation which is inconsistent with what we and others such as Weiner[8,19] have found. Only two conclusions appear to be admissible: (1) the new energy curves are inaccurate or (2) one or both of two selection rules must be abandoned, namely, the "semiclassical" rule which requires that reaction occur only if there is a crossing of a Na $\cdots$ Na energy curve with that of the product ion and the "first-order" rule (2.33), broken by Coriolis forces, which disallows the reaction of Σ^- states. Conclusion (2) seems so unlikely, particularly for the thermal energies at which the rates were measured, that we are forced to conclude that the new energy curves are qualitatively incorrect.

New experimental measurements should permit us to refine our knowledge of the reaction mechanism, regardless of uncertainties about the energy curves. For one thing, AI can be investigated using atoms prepared by circularly polarized light. We already have mentioned an experimental procedure which populates only the Na($3\,^2P_{3/2}$) hyperfine states $M_F=M_F'=3$. By using a circularly polarized laser which intersects each of two crossed beams at an angle $\beta\neq\pi/2$, it is possible to pump one to the hyperfine state $M_F=3$ and the other to $M_F=-3$. This requires the Doppler detuning of a Na D_2-line laser which is then split into two circularly polarized components. Although Weiner has not yet reported an experiment of this sort, a related experiment which he recently performed[19] demonstrates the feasibility of the concept. If the integral cross section were measured for this arrangement we could add another equation to the set (6.3) and thereby obtain a further constraint on the cross section $\sigma_\alpha(E)$. In principle, one could go a step further by measuring the polarization dependence for these state preparations. In experiments of this type the frequency of the laser would be changed as its direction relative to the atomic beam is altered. Thus, by varying the degree of Doppler detuning one could resonantly excite atoms having a selected, fixed value of relative velocity regardless of the direction and polarization of the laser. Experiments of this sort very well might lead to an unambiguous identification of the reactive triplet state.

Other sources of valuable information are measurements of how the polarization dependence of the AI rate varies with the relative velocity of the reactant atoms. These variations not only are intrinsically interesting, they reveal much about the reaction mechanism. Consider, for example, the general observation[2] that with linearly polarized light the polarization dependence of the AI rate diminishes as the relative velocity of the reactants decreases. This immediately suggests that some state with a $\sigma\pi$ configuration plays a dominant role at low energies but is relatively inconsequential at higher energies such as those of Fig. 1. Ideally, one would find that a single state was participating at very low energies and then identify it by its characteristic polarization curve (cf. Fig. 2), but the situation probably is not that simple.

Finally, other, complementary approaches are being developed as tools for extracting information about the reaction mechanism from experimental observations. Of particular interest is a recent study by Wang, de Vries, and Weiner[8] in which the alignment of the angular momentum vector of the product Na_2^+ ion was measured and then used to estimate the relative reactivity of σ^2 and π^2 configurations. All of this illustrates that the "prototypical" associative ionization reaction of two Na($3\,^2P_{3/2}$) atoms exhibits a surprisingly rich behavior. By elucidating its mechanism we shall have learned much that will be transferrable to other systems.

ACKNOWLEDGMENTS

This research was supported by a grant from the National Science Foundation. We thank Professor John Weiner for correspondence from which we have benefitted greatly.

APPENDIX A: PROOF OF THE EXPANSION THEOREM

The expansion theorem (3.24) is not difficult to prove provided that one can make use of two preliminary results which appear below as (A5) and (A7). Accordingly, we first shall prove (A5) and (A7) and then proceed to (3.24). The basic approach is that of Yutsis, Levinson, and Varagas.

1. Two preliminary relationships

(A5) is an expression of the trivial observation that the Clebsch-Gordon coefficient $\langle J_1M_1J_2M_2\,|\,JM\rangle$ is a pure number which has no dependence on the orientations of coordinate systems. By means of the identity

$$\langle J_1M_1J_2M_2\,|\,JM\rangle=\langle J_1M_1J_2M_2\,|\,\underline{R}(\Omega)\underline{R}^\dagger(\Omega)\,|\,J_1J_2JM\rangle \tag{A1}$$

we can connect this CG coefficient to matrix elements of the rotation operator

$$\underline{R}(\Omega)=e^{-i\alpha J_z}e^{-i\beta J_y}e^{-i\gamma J_z} \tag{A2}$$

and to its inverse $\underline{R}^{-1}(\Omega)=\underline{R}^\dagger(\Omega)$, both of which are parametrized by the Euler angles $(\alpha,\beta,\gamma)=\Omega$ defined in the text. With the angular momentum $\mathbf{J}$ identified as the sum of two commuting angular momenta, $\mathbf{J}_1$ and $\mathbf{J}_2$, the rotation operator can be decomposed into the product of two operators, $\underline{R}_1(\Omega)$ and $\underline{R}_2(\Omega)$, one specific to each angular momentum. (A1) then can be written in the form

$$\langle J_1M_1J_2M_2 \mid JM\rangle = \sum_{N_1,N_2,N} \langle J_1N_1J_2N_2 \mid JN\rangle [\mathscr{R}^{J_1}_{N_1M_1}(\Omega)]^* [\mathscr{R}^{J_2}_{N_2M_2}(\Omega)]^* \mathscr{R}^{J}_{NM}(\Omega)$$

$$= \sum_{N_1,N_2,N} (-1)^{N_1-M_1}(-1)^{N_2-M_2} \langle J_1N_1J_2N_2 \mid JN\rangle \mathscr{R}^{J_1}_{-N_1-M_1}(\Omega)\mathscr{R}^{J_2}_{-N_2-M_2}(\Omega)\mathscr{R}^{J}_{NM}(\Omega) . \quad \text{(A3)}$$

From this, the definition (3.5) of the $3j$ symbol, and the relationship $\begin{pmatrix} Q & R & S \\ q & r & s \end{pmatrix} = (-1)^{Q+R+S}\begin{pmatrix} Q & R & S \\ q & r & s \end{pmatrix}$, it follows that

$$\begin{pmatrix} J_1 & J_2 & J \\ -M_1 & -M_2 & M \end{pmatrix}(-1)^{M+M_1+M_2}$$

$$= \sum_{N_1,N_2,N} (-1)^{N_1+N_2+N} \begin{pmatrix} J_1 & J_2 & J \\ -N_1 & -N_2 & N \end{pmatrix}$$

$$\times \mathscr{R}^{J_1}_{-N_1-M_1}(\Omega)\mathscr{R}^{J_2}_{-N_2-M_2}(\Omega)\mathscr{R}^{J}_{NM}(\Omega) . \quad \text{(A4)}$$

The phase factors appearing explicitly in this formula clearly can be discarded and so we arrive at the first of the desired results, namely,

$$\begin{pmatrix} J_1 & J_2 & J \\ M_1 & M_2 & M \end{pmatrix} = \sum_{N_1,N_2,N} \begin{pmatrix} J_1 & J_2 & J \\ N_1 & N_2 & N \end{pmatrix} \mathscr{R}^{J_1}_{N_1M_1}(\Omega)$$

$$\times \mathscr{R}^{J_2}_{N_2M_2}(\Omega)\mathscr{R}^{J}_{NM}(\Omega) . \quad \text{(A5)}$$

To obtain the second we consider a set of commuting angular moments $\{\mathbf{J}_n; n = 1, \ldots, N-1\}$, together with the composite $\mathbf{J} = \sum_{n=1}^{N-1} \mathbf{J}_i$. The next step is insertion of the expression $\underline{R}(\Omega) = \prod_{n=1}^{N-1} \underline{R}_n(\Omega)$ into the formula

$$\prod_{n=1}^{N-1} \mathscr{R}^{J_n}_{M_nM'_n}(\Omega) = \langle J_1M_1, \ldots, J_{N-1}M_{N-1} \mid \underline{R}(\Omega) \mid J_1M'_1, \ldots, J_{N-1}M'_{N-1}\rangle . \quad \text{(A6)}$$

Then, by introducing Eq. (3.9) from the text we obtain the desired formula

$$\prod_{n=1}^{N-1} \mathscr{R}^{J_n}_{M_nM'_n}(\Omega) = \sum_{a,J,M,M'} \langle (J_1 \ldots J_{N-1})aJM' \mid M'_1 \cdots M'_{N-1}\rangle \mathscr{R}^{J}_{MM'}(\Omega) \langle M_1 \cdots M_{N-1} \mid (J_1 \ldots J_{N-1})aJM\rangle . \quad \text{(A7)}$$

A. The expansion theorem

Let us now consider a "standard" JM coefficient,

$$\underline{F}\begin{pmatrix} J_1 & \cdots & J_N \\ M_1 & \cdots & M_N \end{pmatrix},$$

the diagram of which has one arrow on each internal line but no arrows on any of its external lines (cf. Sec. III). $\underline{F}$ has an algebraic expression in terms of $3j$ symbols and this expression includes internal angular momenta (those associated with internal lines) which we label $L_1, \ldots, L_K$.

We replace each $3j$ symbol of $\underline{F}$ using the formula (A5). Now consider the portion of $\underline{F}$ containing L_i $(1 \le i \le K)$. Prior to the use of (A5) this portion was of the form

$$\sum_{m_i} \begin{pmatrix} \cdots & \cdots & L_i \\ \cdots & \cdots & m_i \end{pmatrix}(-1)^{L_i-m_i} \begin{pmatrix} \cdots & \cdots & L_i \\ \cdots & \cdots & -m_i \end{pmatrix} \quad \text{(A8)}$$

to within a phase factor that was independent of m_i. After the application of (A5) this portion of $\underline{F}$ is

$$\sum_{m_i}\sum_{q,q'} \begin{pmatrix} \cdots & \cdots & L_i \\ \cdots & \cdots & q \end{pmatrix}(-1)^{L_i-m_i} \begin{pmatrix} \cdots & \cdots & L_i \\ \cdots & \cdots & q' \end{pmatrix} \mathscr{R}^{L_i}_{qm_i}\mathscr{R}^{L_i}_{q'-m_i}$$

$$= \sum_{m_i}\sum_{q,q'} \begin{pmatrix} \cdots & \cdots & L_i \\ \cdots & \cdots & q \end{pmatrix}(-1)^{L_i+q'} \begin{pmatrix} \cdots & \cdots & L_i \\ \cdots & \cdots & q' \end{pmatrix} \mathscr{R}^{L_i}_{qm_i}[\mathscr{R}^{L_i}_{-q'm_i}]^*$$

$$= \sum_{q} \begin{pmatrix} \cdots & \cdots & L_i \\ \cdots & \cdots & q \end{pmatrix}(-1)^{L_i-q} \begin{pmatrix} \cdots & \cdots & L_i \\ \cdots & \cdots & -q \end{pmatrix} . \quad \text{(A9)}$$

Therefore, the parts of the algebraic expression for $\underline{F}$ which are associated with its internal lines are not altered by the use of (A5). This leaves us free to write

$$\underline{F}\begin{pmatrix} J_1 & \cdots & J_N \\ M_1 & \cdots & M_N \end{pmatrix} = \sum_{Q_1,\ldots,Q_N} \underline{F}\begin{pmatrix} J_1 & \cdots & J_N \\ Q_1 & \cdots & Q_N \end{pmatrix} \mathscr{R}^{J_1}_{Q_1M_1}(\Omega) \cdots \mathscr{R}^{J_N}_{Q_NM_N}(\Omega) . \quad \text{(A10)}$$

We next act upon both sides of this equation with the identity operator $(8\pi^2)^{-1}\int d\Omega$. The integral of the product of representation coefficients appearing on the right-hand side of (A10) is evaluated using (A7),

$$
\begin{aligned}
&(8\pi^2)^{-1}\int d\Omega \mathscr{R}^{J_1}_{Q_1M_1}(\Omega)\cdots\mathscr{R}^{J_N}_{Q_NM_N}(\Omega)\\
&\quad=(8\pi^2)^{-1}\sum_{a,J,M,M'}\int d\Omega \mathscr{R}^{J*}_{-M-M'}(\Omega)\mathscr{R}^{J_N}_{Q_NM_N}(\Omega)(-1)^{M-M'}\\
&\qquad\qquad\times\langle(J_1\cdots J_{N-1})aJM\mid Q_1\cdots Q_{N-1}\rangle\langle M_1\cdots M_{N-1}\mid(J_1\cdots J_{N-1})aJM'\rangle\\
&\quad=\sum_a[J_N]^{-1}(-1)^{-Q_N+M_N}\langle(J_1\cdots J_{N-1})aJ_N-Q_N\mid M'_1\cdots M'_{N-1}\rangle\langle M_1\cdots M_{N-1}\mid(J_1\cdots J_{N-1})aJ_N-M_N\rangle\ .
\end{aligned}
\tag{A11}
$$

This can be written in a more symmetric form by observing that $(-1)^{2J_N}=(-1)^{2M_N}$. Consequently, the result of acting upon (A10) with the integral identity operator is the separation formula

$$
\underline{F}\begin{bmatrix}J_1&\cdots&J_N\\M_1&\cdots&M_N\end{bmatrix}=(-1)^{J_N-M_N}\sum_a R(a)\langle M_1\cdots M_{N-1}\mid(J_1\cdots J_{N-1})aJ_N-M_N\rangle\ ,
\tag{A12}
$$

wherein

$$
\begin{aligned}
R(a)&=[J_N]^{-1}\sum_{Q_1,\ldots,Q_N}\underline{F}\begin{bmatrix}J_1&\cdots&J_N\\Q_1&\cdots&Q_N\end{bmatrix}\langle(J_1\cdots J_{N-1})aJ_N-Q_N\mid Q_1\cdots Q_{N-1}\rangle(-1)^{J_N-Q_N}\\
&=[J_N]^{-1}\sum_{Q_1,\ldots,Q_N,Q}\underline{F}\begin{bmatrix}J_1&\cdots&J_N\\Q_1&\cdots&Q_N\end{bmatrix}\begin{bmatrix}J_N\\QQ_N\end{bmatrix}\langle(J_1\cdots J_{N-1})aJ_NQ\mid Q_1\cdots Q_{N-1}\rangle\ .
\end{aligned}
\tag{A13}
$$

To complete the story we now examine the special cases of $N=3$, 2, and 1. For $N=3$ the result is

$$
\underline{F}\begin{bmatrix}J_1&J_2&J_3\\M_1&M_2&M_3\end{bmatrix}=(-1)^{J_3-M_3}\langle M_1M_2\mid J_3-M_3\rangle R\ ,
\tag{A14}
$$

with

$$
R=\sum_{\substack{Q_1,Q_2,\\Q_3}}\underline{F}\begin{bmatrix}J_1&J_2&J_3\\Q_1&Q_2&Q_3\end{bmatrix}\langle J_3-Q_3\mid Q_1Q_2\rangle(-1)^{J_3-Q_3}\frac{1}{[J_3]}\ .
\tag{A15}
$$

These two equations can be rewritten in the form

$$
\underline{F}\begin{bmatrix}J_1&J_2&J_3\\M_1&M_2&M_3\end{bmatrix}=R'\begin{bmatrix}J_1&J_2&J_3\\M_1&M_2&M_3\end{bmatrix}\ ,
\tag{A14'}
$$

where

$$
R'=\sum_{\substack{Q_1,Q_2,\\Q_3}}\underline{F}\begin{bmatrix}J_1&J_2&J_3\\Q_1&Q_2&Q_3\end{bmatrix}\begin{bmatrix}J_1&J_2&J_3\\Q_1&Q_2&Q_3\end{bmatrix}\ .
\tag{A15'}
$$

For the case of

$$
\underline{F}\begin{bmatrix}J_1&J_2\\M_1&M_2\end{bmatrix}\ ,
$$

it is simplest to proceed directly from (A10). Integrating directly, we find

$$
\begin{aligned}
\underline{F}\begin{bmatrix}J_1&J_2\\M_1&M_2\end{bmatrix}&=\sum_{Q_1,Q_2}(-1)^{Q_2-M_2}\frac{1}{[J_2]}\underline{F}\begin{bmatrix}J_1&J_2\\Q_1&Q_2\end{bmatrix}\delta_{Q_1,-Q_2}\delta_{M_1,-M_2}\delta_{J_1,J_2}\\
&=(-1)^{J_1-M_2}\delta_{J_1J_2}\delta_{M_1-M_2}\frac{1}{[J_1]}\sum_{Q_1}(-1)^{J_1+Q_1}\underline{F}\begin{bmatrix}J_1&J_1\\Q_1&-Q_1\end{bmatrix}\\
&=\delta_{J_1J_2}\begin{bmatrix}J_1\\M_1\quad M_2\end{bmatrix}\frac{1}{[J_2]}\sum_{Q,Q_1}\begin{bmatrix}J_1\\Q_1\quad Q\end{bmatrix}\underline{F}\begin{bmatrix}J_1&J_1\\Q_1&Q\end{bmatrix}\ .
\end{aligned}
\tag{A16}
$$

TABLE V. Density-matrix Legendre polynomial coefficients defined by (B6). The first column identifies the state (labeled as in Table I), its MO configuration, and its term symbol. The second-column labels o, e, and t indicate sums of $\rho_{xx}(\mathscr{I},\mathscr{S})$ over odd (o), even (e), and all (t) values of the nuclear spin quantum number $\mathscr{I}$. These results are specific to the case of *linear* polarization. An entry such as 1.534[−2] indicates a numerical value of 1.534×10^{-2}. The triplet-state entries labeled c are specific to *circular* polarization and refer to the single value of $\mathscr{I}=3$. The column headings $T=0,2,4$ indicate the degrees of the Legendre polynomials. Finally, in the case of the $^3\Pi_u$ state labeled h there is an additional row marked c'. The c' entries in the columns headed $T=0$ and 2 are coefficients for $T=1$ and 3, respectively. The upper signs are specific to the state (cf. Table I) involving the orbital π_u^1 and the lower signs to the state involving π_u^{-1}.

Triplet states		$T=0$	$T=2$	$T=4$
b	o	6.8780[−2]	8.9976[−2]	1.4618[−2]
$\sigma_g\sigma_u$	e	2.1958[−2]	3.1720[−2]	4.4300[−3]
$^3\Sigma_u^+$	t	9.0738[−2]	1.2170[−1]	1.9048[−2]
	c	1.3330[−1]	−1.9047[−1]	5.7140[−2]
d	o	3.1582[−2]	−1.2188[−2]	0
π_g^2	e	2.9377[−2]	−1.2503[−2]	0
$^3\Sigma_g^-$	t	6.0959[−2]	−2.4691[−2]	0
	c	0	0	0
f	o	5.4399[−2]	−3.1544[−2]	7.3088[−3]
$\pi_g\pi_u$	e	2.9377[−2]	−2.4894[−2]	2.2150[−3]
$^3\Sigma_u^+$	t	8.3776[−2]	−5.6438[−2]	9.5240[−3]
	c	6.6660[−2]	−9.5238[−2]	2.8572[−2]
h	o	8.3170[−2]	2.9216[−2]	−1.4618[−2]
$\sigma_g\pi_u$	e	1.5135[−2]	3.4127[−2]	−4.4300[−3]
$^3\Pi_u$	t	9.8305[−2]	3.2629[−2]	−1.9408[−2]
	c	2.0000[−2]	−1.4286[−1]	−5.7143[−2]
	c'	±2.0000[−2]	∓2.0000[−1]	
j	o	3.1582[−2]	6.0942[−3]	0
$\sigma_g\pi_g$	e	2.9377[−2]	6.2517[−3]	0
$^3\Pi_g$	t	6.0959[−2]	1.2346[−2]	0
	c	0	0	0

Singlet states		$T=0$	$T=2$	$T=4$
a	o	1.534[−2]	2.065[−2]	3.125[−3]
σ_g^2	e	1.490[−2]	1.991[−2]	3.134[−3]
$^1\Sigma_g^+$	t	3.025[−2]	4.056[−2]	6.349[−3]
c	o	2.2719[−2]	−1.7831[−2]	1.6076[−3]
π_g^2	e	2.2490[−2]	−1.7440[−2]	1.5671[−3]
$^1\Sigma_g^+$	t	4.5209[−2]	−3.5270[−2]	3.1747[−3]
e	o	2.0010[−2]	−1.2189[−2]	0
$\pi_g\pi_u$	e	1.7802[−2]	−1.2503[−2]	0
$^1\Sigma_u^-$	t	3.7812[−2]	−2.4692[−2]	0
g	o	2.0010[−2]	6.0942[−3]	0
$\sigma_g\pi_u$	e	1.7802[−2]	6.2517[−3]	0
$^1\Pi_u$	t	3.7812[−2]	1.2326[−3]	0
i	o	7.9698[−3]	1.4015[−3]	−3.2152[−3]
$\sigma_g\pi_g$	e	7.3084[−3]	1.2350[−3]	−3.1341[−3]
$^1\Pi_g$	t	1.5278[−2]	2.6455[−3]	−6.3493[−3]

Similarly for $N=1$, the result of integrating (A10) is

$$\underline{F}\begin{bmatrix} J_1 \\ M_1 \end{bmatrix} = \underline{F}\begin{bmatrix} J_1 \\ Q_1 \end{bmatrix} \delta_{J_1,0}\delta_{Q_1,0} \ . \tag{A17}$$

Diagrams corresponding to (A14'), (A16), and (A17) are given in Eq. (3.28) of the text.

APPENDIX B: COMPUTATION OF DENSITY MATRIX

Summarized here is the procedure for computing density-matrix elements, $\rho_{xx'}(\mathscr{I}\mathscr{S},\hat{\alpha})$, connected with the associative ionization of two $\mathrm{Na}((3p)^2P)$ atoms. The nuclei are assumed to be identical and the system is treated in the quasi-two-electron approximation.

The first task is to evaluate the integrals

$$(\mathscr{S}x \mid \mathscr{S}t) = (x;\mathscr{S}\Omega_{\mathscr{S}}\mathscr{I}\Omega_{\mathscr{I}} \mid t;\mathscr{S}\Omega_{\mathscr{S}}\mathscr{I}\Omega_{\mathscr{I}}) \ , \tag{B1}$$

which occur in the density matrix formula (4.4). In the quasi-two-electron approximation the unit normalized ket $\mid t;\mathscr{S}\Omega_{\mathscr{S}}\mathscr{I}\Omega_{\mathscr{I}})$ has the form

$$\mid t;\mathscr{S}\Omega_{\mathscr{S}}\mathscr{I}\Omega_{\mathscr{I}}) = 2^{-1/2} \mid \mathscr{I}\Omega_{\mathscr{I}}) \mid \mathscr{S}\Omega_{\mathscr{S}})[\mid nL\Omega;A) \mid n'L'\Omega';B) + (-1)^{\mathscr{S}} \mid n'L'\Omega';B) \mid nL\Omega;A)] \ . \tag{B2}$$

The convention used here and throughout this appendix is that the first (left most) ket of the product $\mid a) \mid b)$ is specific to electron 1 and the second (right most) to electron 2. The atomic orbitals (AO's) appearing here are orthonormal eigenstates of one-electron energy operators which include pseudopotentials representative of the "core electrons." The letters A and B identify the two identical nuclei upon which these orbitals are centered.

The symbol $\mid x;\mathscr{S}\Omega_{\mathscr{S}}\mathscr{I}\Omega_{\mathscr{I}})$ denotes a molecular-type, two-electron ket defined in the asymptotic ($R\rightarrow\infty$) limit. It can be written in terms of the primitive molecular orbitals (MO's)

$$\mid \eta\lambda\omega p) \equiv \mid \omega p) = \mid \omega;A) + p \mid \omega;B) \ . \tag{B3}$$

Here p [equal either to 1 (gerade) or to -1 (ungerade)] is the parity of this orbital and ω is the projection quantum number of electronic orbital angular momentum in the direction $\mathbf{k}$ (which in the asymptotic region is opposite to the direction of the internuclear axis). η and λ are labels that complete the identifications of the AO's. The two-electron ket now can be written in the form

$$\begin{aligned} \mid x;\mathscr{S}\Omega_{\mathscr{S}}\mathscr{I}\Omega_{\mathscr{I}}) = (2N_x)^{-1/2} \mid \mathscr{I}\Omega_{\mathscr{I}}) \mid \mathscr{S}\Omega_{\mathscr{S}}) \\ \times \{\tfrac{1}{2}[\mid \omega p) \mid \omega' p') - \mid \omega - p) \mid \omega' - p')] \\ + (-1)^{\mathscr{S}} \tfrac{1}{2}[\mid \omega' p') \mid \omega p) \\ - \mid \omega' - p') \mid \omega - p)]\} \ , \end{aligned} \tag{B4}$$

with ω and ω' so chosen that $\omega+\omega'=\Lambda_x$ and p and p' such that their product equals the parity of the molecular state. The quantity $\frac{1}{2}[\mid \omega p) \mid \omega' p') - \mid \omega - p) \mid \omega' - p')]$ is the "covalent part" of the MO product state $\mid \omega p) \mid \omega' p')$, that is, the part of this state which is devoid of ionic (A^+B^- or A^-B^+) character. Finally, the numerical factor $N_x = 2[1+\delta(\omega \mid \omega')]$ insures that the two-electron ket is unit normalized.

It is a direct consequence of these definitions that (with $n\lambda = nL$ and $\eta'\lambda' = n'L'$),

$$\begin{aligned} (\mathscr{S}x \mid \mathscr{S}q) = N_x^{-1/2}[p'\delta(\omega \mid \Omega)\delta(\omega' \mid \Omega') \\ + (-1)^{\mathscr{S}} p\delta(\omega \mid \Omega;)\delta(\omega' \mid \Omega)] \ . \end{aligned} \tag{B5}$$

Consequently, the density-matrix Legendre polynomial coefficients defined by (5.5) may be written as

$$\begin{aligned} \rho^T_{xy}(\mathscr{I}\mathscr{S}) = (N_xN_y)^{-1/2}[p'_xp'_y(\omega_x\omega'_x \mid \rho^T(\mathscr{I}\mathscr{S}) \mid \omega_y\omega'_y) + (-1)^{\mathscr{S}} p'_xp_y(\omega_x\omega'_y \mid \rho^T(\mathscr{I}\mathscr{S}) \mid \omega'_y\omega_y) \\ + (-1)^{\mathscr{S}} p_xp'_y(\omega'_x\omega_x \mid \rho^T(\mathscr{I}\mathscr{S}) \mid \omega_y\omega'_y) + p_xp_y(\omega'_x\omega_x \mid \rho^T(\mathscr{I}\mathscr{S}) \mid \omega'_y\omega_y)] \ , \end{aligned} \tag{B6}$$

wherein

$$\begin{aligned} (\Omega\Omega' \mid \rho^T(\mathscr{I}\mathscr{S}) \mid \tilde{\Omega}\,\tilde{\Omega}') \\ = \sum_{\mathscr{L}\mathscr{L}'} a(T0,LL',\mathscr{L}\mathscr{L}',\{\Omega\}) \\ \times \sum_{M_F,M'_F} P(M_F,M'_F) g(T0,\Gamma,\mathscr{L}\mathscr{L}',M_FM'_F) \ . \end{aligned} \tag{B7}$$

The quantities a and g appearing in the last of these formulas are given by (4.12) and (4.25), respectively. The first of these is trivial to evaluate. The second involves readily computable $6j$ and $9j$ symbols. The state populations $P(M_F,M'_F)$ which contribute to the quantities defined by (B7) have been treated by Hertel and Stoll;[10,11] formulas appropriate to circularly and linearly polarized light are given by their Eqs. (52) and (58), respectively. Numerical results for the the states of Table I are presented in Table V.

[1]J. G. Kircz, R. Morgenstern, and G. Nienhius, Phys. Rev. Lett. **48**, 610 (1982).

[2]H. A. J. Meyer, H. P. v. d. Meulen, R. Morgenstern, I. V. Hertel, E. Meyer, H. Schmidt, and R. White, Phys. Rev. A **33**, 1421 (1986).

[3]E. W. Rothe, R. Theyunni, C. P. Peck, and C. C. Tung, Phys. Rev. A **31**, 1362 (1985); **33**, 1426 (1986).

[4]D. M. Jones and J. S. Dahler, Phys. Rev. A **31**, 210 (1985).

[5]R. J. Bieniek, Phys. Rev. A **18**, 392 (1978); see also W. H. Miller, C. A. Slocomb, and H. F. Schaeffer III, J. Chem. Phys. **56**, 1347 (1972); J. N. Bardsley, J. Phys. B **1**, 349 (1968); A. P. Hickman and H. Morgner, *ibid.* **9**, 1765 (1976).

[6]H. P. Saha, J. S. Dahler, and S. E. Nielsen, Phys. Rev. A **28**, 1487 (1983).

[7]H. P. Saha, J. S. Dahler, and D. M. Jones, Phys. Rev. A **30**, 1345 (1984).

[8]M.-X. Wang, M. S. de Vries, and J. Weiner, Phys. Rev. A **34**, 1869 (1986).

[9]G. Nienhuis, Phys. Rev. A **26**, 3137 (1982).

[10]I. V. Hertel and W. Stoll, Adv. At. Mol. Phys. **1**, 113 (1978); A. Fischer and I. V. Hertel, Z. Phys. A **304**, 103 (1982); see also J. Macek and I. V. Hertel, J. Phys. B **7**, 2173 (1974); I. V. Hertel and W. Stoll, *ibid.* **7**, 583 (1974).

[11]I. V. Hertel and W. Stoll, Adv. At. Mol. Phys. **13**, 113 (1977); see especially Sec. III, and the references cited therein.

[12]D. M. Jones and J. S. Dahler (unpublished).

[13]This modification results from symmetrizing the total wave function to account for nuclear statistics. One must also remember that the observed state of the product ion is symmetrized with respect to nuclear permutation.

[14]This is to be distinguished from the similar projection along $\hat{\mathbf{R}}$, given initially (long before the collision) by $-\Lambda_x = -\Lambda_p$.

[15]A. P. Yutsis, I. B. Levinson, and V. V. Varagas, *The Theory of Angular Momentum* (Israel Program for Scientific Translations, Jerusalem, 1962) [Distributed by Old Bourne Press, London]. See also E. El Baz and B. Castel, *Graphical Methods of Spin Algebras in Atomic, Nuclear, and Particle Physics* (Marcel Dekker, New York, 1972). The presention of Sec. III is adapted from Yutsis, Levinson, and Varagas.

[16]A. Messiah, *Quantum Mechanics* (Wiley, New York, 1958). The $6j$ and $9j$ symbols used here are defined as in Appendix C of this book.

[17]R. Mortagnani, P. Riani, and Ol. Salvetti, Theor. Chim. Acta **64**, 431 (1984).

[18]A. Henriet and F. Masnou-Seeuws, J. Phys. B **20**, 671 (1987).

[19]M.-X. Wang, M. S. de Vries, J. Keller, and J. Weiner, Phys. Rev. A **32**, 687 (1985).

[20]A. Henriet, F. Masnou-Seeuws, and C. LeSech, Chem. Phys. Lett. **118**, 507 (1985).